

CHARLES UNIVERSITY IN PRAGUE

FACULTY OF SCIENCE

Study programme: Analytical chemistry



Mgr. Anna Kubíčková

Analysis of amino acids and polyamines by HPLC and CZE

DISSERTATION THESIS

Supervisor: Doc. RNDr. Pavel Coufal, Ph.D.

Prague, 2011

This thesis summarizes the results obtained in the years 2007–2011 during my Ph.D. studies at the Department of Analytical Chemistry, Faculty of Science of the Charles University in Prague.

The work was financially supported by the Grant Agency of the Charles University in Prague (project SVV 2011-263204) and by the Ministry of Education, Youth and Sports of the Czech Republic projects (long-term project MSM0021620857).

Supervisor: Doc. RNDr. Pavel Coufal, Ph.D.
Department of Analytical Chemistry
Faculty of Science, Charles University in Prague

Supervisor – consultant: Doc. RNDr. Zuzana Bosáková, CSc.
Department of Analytical Chemistry
Faculty of Science, Charles University in Prague

I declare that all the results used and published in this thesis have been obtained by my own experimental work, supervised by Doc. RNDr. Pavel Coufal, Ph.D., all the references are properly cited and this thesis has not been applied to obtain the same or other academic degree.

Prague, 25.10. 2011

Mgr. Anna Kubičková

ABSTRACT (EN)

This work is focused on two specific classes of amines. First group comprises of cyclic polyaminocarboxylates from the DOTA (1,4,7,10-tetraazacyclododecane-1,4,7,10-tetraacetic acid) family, which are important reaction intermediates in magnetic resonance imaging (MRI) contrast agent synthesis. In the development of new contrast agents, carboxyl groups are very often protected with *tert*-butyl ester groups. Among these derivatives, *t*Bu₃DO3A is of the highest importance. Therefore, reverse-phase high performance liquid chromatographic (RP-HPLC) and non-aqueous capillary zone electrophoretic (CZE) methods were evaluated for qualitative and quantitative analysis of *t*Bu₃DO3A (1,4,7,10-tetraazacyclododecan-1,4,7-tris(*tert*-butylacetate) and two typical reaction by-products, i.e. *t*Bu₄DOTA (1,4,7,10-tetraazacyclododecan-1,4,7,10-tetrakis(*tert*-butylacetate) and *t*Bu₂DO2A (1,4,7,10-tetraazacyclododecan-1,4-bis(*tert*-butylacetate). These optimized methods were successfully applied to monitoring of real reaction mixtures during synthesis of a new MRI contrast agent. No further sample pretreatment was necessary.

In the second part of the thesis, proteinogenic amino acids and polyamines were used as model analytes for development of a new post-column solid-phase reactor suitable for on-line derivatization in HPLC. The solid-phase reactor is filled with fine copper(II) oxide powder. Passage of the analytes through the reactor leads to formation of copper(II) complexes. Unlike free amino acids and polyamines, the copper(II) complexes show significant absorbance in UV region and accordingly detection sensitivity of amino acids increases by two to four orders of magnitude when compared to analyses without the derivatization step. The increase of the detector response for the polyamines is from one to two orders of magnitude. The presented solid-phase reactor brings simple, inexpensive and versatile solution for UV-VIS detection of coordinating compounds, which do not normally absorb well in the UV-VIS region.

ABSTRAKT (CZ)

V rámci této disertační práce byly studovány dvě skupiny aminů. První z nich tvoří deriváty cyklického polyaminokarboxylátu DOTA (kyselina 1,4,7,10-tetraazacyklododekan-1,4,7,10-tetraoctová), které jsou významnými reakčními meziprodukty při syntéze kontrastních látek pro magnetickou rezonanci (MRI). Výsadní postavení mezi těmito deriváty zaujímá *t*Bu₃DO3A (1,4,7,10-tetraazacyklododekan-1,4,7-tris(*tert*-butylacetát)). Vedle *t*Bu₃DO3A byly detailně studovány dva typické vedlejší produkty syntézy *t*Bu₃DO3A, tj. *t*Bu₄DOTA (1,4,7,10-tetraazacyklododekan-1,4,7,10-tetrakis(*tert*-butylacetát)) a *t*Bu₂DO2A (*t*Bu₂DO2A, i.e. 1,4,7,10-tetraazacyklododekan-1,4-bis(*tert*-butylacetát)). Ke studiu výše zmíněných látek byla použita kapalinová chromatografie v reverzním módu (RP-HPLC) a kapilární zónová elektroforéza (CZE) s UV-VIS detekcí. Vyvinuté metody byly prakticky otestovány na analýze reálných reakčních směsí. Lze konstatovat, že obě metody představují rychlé, účinné a jednoduché řešení pro sledování syntézy nově vyvíjených MRI kontrastních látek, neboť mohou být použity přímo, bez jakékoli další předúpravy vzorků reakčních směsí.

Druhá část této práce se věnuje problému detekce polyaminů a aminokyselin běžnou UV-VIS spektrometrií. Byl vyvinut a otestován nový “solid-phase” reaktor na bázi oxidu měďnatého vhodný pro on-line derivatizaci aminů v HPLC. Při průchodu analytů tímto reaktorem dochází k vytvoření měďnatého komplexu daného aminu. Na rozdíl od volných aminů vykazují jejich měďnaté komplexy silný absorpční pás v UV oblasti, čehož lze s výhodou využít pro jejich citlivou spektrofotometrickou detekci. Citlivost detekce proteinogenních aminokyselin vzrostla při použití “solid-phase” reaktoru o dva až čtyři řády. V případě polyaminů byl nárůst citlivosti o něco nižší, jeden až dva řády, ale stále významný. Derivatizace aminů “solid-phase” reaktorem na bázi oxidu měďnatého a následná UV-VIS detekce představuje univerzální, jednoduchou a ekonomickou alternativu sofistikovaných a drahých metod detekce.

TABLE OF CONTENTS

ABSTRACT (EN)	4
ABSTRAKT (CZ)	5
TABLE OF CONTENTS	6
LIST OF ABBREVIATIONS AND SYMBOLS	8
1. PREFACE	11
2. SEPARATION OF CYCLEN DERIVATIVES	15
2.1 Introduction	15
2.2 Experimental	19
2.2.1 Chemicals	19
2.2.2 Synthesis	19
2.2.3 HPLC instrumentation and conditions	22
2.2.4 CZE instrumentation and conditions	23
2.3 Results and discussion	24
2.3.1 HPLC method development	24
2.3.2 CZE method development	26
2.3.3 Quantification	27
2.3.4 Applications in the syntheses of <i>t</i> Bu ₃ DO3A and PiB- <i>t</i> Bu ₃ DO3A	34
2.4 Conclusion	38
3. SOLID-PHASE DERIVATIZATION IN HPLC	40
3.1 Introduction	40
3.1.1 Derivatization in HPLC	40
3.1.2 Amino acids	42
3.1.3 Applicability study	45
3.2 Experimental	47
3.2.1 Chemicals	47
3.2.2 UV-VIS measurements	48
3.2.3 HPLC instrumentation and conditions	48

3.3 Results and discussion	51
3.3.1 Amino acids derivatization	51
3.3.2 Applicability study	60
3.4 Conclusion	68
REFERENCES	70
ACKNOWLEDGEMENT	75
LIST OF PUBLICATIONS	76
DECLARATION OF CO-AUTHORS	78
APENDIX 1: A. Kubíčková, et al.: <i>J. Sep. Sci.</i> 34 (2011), DOI 10.1002/jssc.201100561.	80
APENDIX 2: A. Hamplová et. al. <i>J. Sep. Sci.</i> 33 (2010) 658.	86

LIST OF ABBREVIATIONS AND SYMBOLS

ACN	acetonitrile
AQC	6-aminoquinolyl-N-hydroxysuccinimidyl carbamate
BGE	background electrolyte
CD	conductivity detector
CEC	capillary electrochromatography
CGE	capillary gel electrophoresis
CLC	capillary liquid chromatography
CLD	chemiluminescent detector
cyclam	1,4,8,11-tetraazacyclotetradecane
cyclen	1,4,7,10-tetraazacyclododecane
CZE	capillary zone electrophoresis
dansyl	(5-dimethylamino)naphthalene-1-sulphonyl chloride
DIEN	bis(2-aminoethyl)amine
DO2A	1,4,7,10-tetraazacyclododecane-1,4-diacetic acid
DO3A	1,4,7,10-tetraazacyclododecane-1,4,7-triacetic acid
DOTA	1,4,7,10-tetraazacyclododecane-1,4,7,10-tetraacetic acid
DTPA	diethylenetriaminepentaacetic acid
ECD	electrochemical detection
EDTA	disodium ethylenediaminetetraacetate
ELSD	evaporative light scattering detector
EN	1,2-diaminoethane
Fmoc	9-fluorenylmethylchloroformate
GABA	γ -aminobutyric acid
GC	gas chromatography
HETP	height equivalent to a theoretical plate
HPLC	high performance liquid chromatography
ICP-EAS	inductively coupled plasma atomic emission spectroscopy
I.D.	inner diameter
LIF	laser-induced fluorescence

LOD	limit of detection
LOQ	limit of quantification
MEKC	micellar electrokinetic chromatography
MRI	magnetic resonance imaging
MS	mass spectrometry
MS/MS	tandem mass spectrometry
NMR	nuclear magnetic resonance
NOTA	1,4,7-triazacyclononane-1,4,7-triacetic acid
OPA	<i>o</i> -phthalaldehyd
PET	positron emission tomography
PiB	Pittsburgh compound B
PITC	phenylisothiocyanate
RID	refractive index detector
RSD	relative standard deviation
SD	standard deviation
SPECT	single photon emission computed tomography
TACN	1,4,7-triazacyclononane
<i>t</i> Bu ₂ DO2A	1,4,7,10-tetraazacyclododecan-1,4-bis(<i>tert</i> -butylacetate)
<i>t</i> Bu ₃ DO3A	1,4,7,10-tetraazacyclododecan-1,4,7-tris(<i>tert</i> -butylacetate)
<i>t</i> Bu ₄ DOTA	1,4,7,10-tetraazacyclododecan-1,4,7,10-tetrakis(<i>tert</i> -butylacetate)
TEA	triethylamine
TETA	1,4,8,11-tetraazacyclotetradecane-1,4,8,11-tetraacetic acid
TFA	trifluoroacetic acid
TLC	thin layer chromatography
TRIS	tris(hydroxymethyl)aminomethane
UV-VIS	ultraviolet and visible region of light spectrum
<i>a</i>	calibration line intercept
<i>A</i>	peak area
<i>b</i>	calibration line slope
<i>c</i> _L	ligand concentration

c_M	metal concentration
h	peak height
i	linearity factor
r	correlation coefficient
t_{mig}	migration time
t_{ret}	retention time
v/v	volume ratio
λ	detection wavelength

1 PREFACE

Amines represent very wide and miscellaneous group of compounds. The overall accepted definition describes amines as derivatives of ammonia, where one or more hydrogen atoms are substituted with an alkyl or aryl group [1]. Such definition covers millions of compounds from simple organic derivatives to biological active compounds like enzymes. This work was focused on two specific groups of amines – polyamines (both linear and cyclic) and amino acids.

There are no doubts about the importance of both these groups. Amino acids is a group of compounds that play very significant role in our everyday life. There are many types of amino acids and lots of them have important biological functions. Above all, there are twenty proteinogenic amino acids, which are elementary building blocks of proteins and therefore essential components of our body. Human body is capable to synthesize only twelve of twenty proteinogenic amino acids from other compounds. The rest of them, namely leucine, isoleucine, valine, phenylalanine, threonine, tryptophan, methionine and lysine, are called essential and have to be obtained from a diet. The amount required differs for adults and children and also depends on the age and life style of the individual. Therefore, amino acids are deeply studied not only by chemist, but also by physicians and nourishment specialists. Apart from these proteinogenic amino acids, there are many other amino acids that can be found in human body. Just briefly few examples: homocysteine is a metabolite of methionine; carnitine, which plays an important role in a transport of fatty acids into mitochondria; ornithine is one of the intermediates in urea cycle; the neurotransmitter GABA (γ -aminobutyric acid) and a hormone of thyroid thyroxine. Moreover, the proportion of certain amino acid in human plasma, saliva or urine is often monitored for diagnostic purposes, because a disbalance of amino acids can indicate several diseases [2 – 3]. There are many areas, where amino acids play important role, besides their biogenic functions and it is almost impossible to give a complete list of them. Just briefly: food industry and nutrition, agriculture, pharmacology, catalysis etc.

Amino acids have employed chemists for more than 200 years yet, as the first one, asparagine, was isolated in 1806 from asparagus sprout. Then a discovery of leucine, cysteine, glycine, and glutamate followed. All the twenty proteinogenic amino acids were described in the first half of the 20th century [4]. Since that time, the various properties of amino acids were studied in great depth. However, the analyses were exacting and time consuming work. That changed after introduction of partition chromatography into analytical chemistry by A.J.P. Martin and R.L.M. Synge [5] and their successors S. Moore, W.H. Stein and D.H. Spackman in 1950th [6]. Another method suitable for studying of amino acids, capillary zone electrophoresis, was introduced in 1960th. Nowadays, amino acids belong to the most extensively studied class of compounds. In the last ten years, more than 70,000 papers dealing with this topic were published with increasing number of papers each year.

The second group of compounds of interest is represented by polyamines. Polyamines are important mainly due to their chelating properties given by presence of a lone electron pair at every nitrogen atom. A complex is formed through sharing these lone electron pairs of a ligand with a central metal atom. There are many areas, where N-containing coordination compounds play an irreplaceable role [7]. First of all, many chelators are natural components of a human body or plants. One should mention porphyrins like for example hem, which serve as a cofactor of the protein hemoglobin, or green pigment chlorophyll, which is essential for photosynthesis.

From other industrial applications it is necessary to mention catalysis [7]. Catalysts are substances that accelerate the rates of chemical reactions. They participate in the chemical reaction but they are not consumed by the reaction itself. Metals and metal complexes are widely used for this purpose, especially for redox reactions like for example hydrogenation. Ligands in the complexes could considerably influence the approach of a substrate to the active metal center and change the properties of the catalyst such as stereoselectivity, solubility, etc. Another field of application is a detoxification. Chelators are capable of converting toxic metals into inert complexes that are excreted from body without any harmful effects. Such behaviour is widely used for wastewater treatment or in case of poisoning with

heavy metals. The most widely used ligands for this objective are EDTA and DOTA [8] (for the structures see Figure 13, page 46).

Medicinal applications of chelates became very important during the last 20 years. Apart from an above mentioned detoxification, coordination compounds are widely used as the carriers of (mostly) toxic metal ions necessary for a medical treatment. The major field of application of chelators in medicine is as contrast agents for magnetic resonance imaging (MRI) [9 – 10], positron emission tomography (PET) [11 – 12] and single photon emission computed tomography (SPECT) [13]. In the last ten years, MRI became routine imaging tool in medical diagnostics. MRI is based on measurement of the signals corresponding to water protons in strong magnetic field. Since tissues differ in amount of water, it is possible to visualize detailed internal structures of a studied body area. Moreover, MRI provides an excellent spatial resolution and therefore is very suitable for imaging of soft tissues like inner organs, tumors and muscles. Unlike MRI, PET and SPECT are based on measurements of emitted radiation (photons from positron-electron annihilation in case of PET and gamma rays in case of SPECT). When compared with MRI, both these methods provide worse spatial resolution. On the other hand, both PET and SPECT surpass MRI in a low consumption of a contrast agent necessary for one scan.

For all the three above mentioned imaging methods, contrast agents based on metal complexes are utilized. The contrast agents require exceptionally stable complexes from thermodynamic point of view as well as from kinetic point of view. Polyamines, especially cyclic ones, are perfectly suitable ligands for this purpose due to their polydentate character and therefore low risk of release of a harmful metal. Nowadays, mainly Gd(III) complexes are used as MRI contrast agents. Various polyamines chelators were prepared and tested for the purpose of MRI contrast agents. The leading ones are ligands from the DOTA and DTPA family (for the structures see Figure 13, page 46). For the PET and SPECT scanning, contrast agents based on radionuclids (for example ^{99}Tc , ^{62}Cu or ^{68}Ga) are utilized. Since radionuclids differ in the ionic radius, it is impossible to find one universal ligand for all of them. From the most often used ligands for PET and SPECT contrast agents one should mention analogues of NOTA, DOTA and TETA (for the

structures see Figure 13, page 46). The latest research is aimed at so called targeted contrast agents and therapy. Molecule of such contrast agent contains a moiety, which binds specifically to certain type of tissue (bones, tumors, etc.), which enables to lower dose of a contrast agent necessary for making a scan.

Aims of the thesis

This work was focused on separation and detection of two classes of amines, i. e. amino acids and polyamines. HPLC and CZE with UV-VIS detection were chosen for this purpose as they represent common instrumentation of a chemical laboratory. Cyclic polyaminocarboxylates from the DOTA family, which are important reaction intermediates in magnetic resonance imaging (MRI) contrast agent synthesis, were studied in order to enable monitoring of the novel MRI contrast agent synthesis. Detection emerged as a major problem of the amino acids and polyamines analysis. Therefore special attention was paid to problems associated with a detection of UV-VIS almost non-absorbing compounds such are amino acids and polyamines.

2 SEPARATION OF CYCLEN DERIVATIVES

2.1 Introduction

MRI is one of the molecular imaging methods routinely used to visualize morphological and physiological changes in body tissues. In this method, contrast agents [14] are utilized to amplify the contrast and resolution between pathological and normal tissues. The contrast agents are often based on transition metal or lanthanide ions. The most widespread are based on the Gd(III) ion, which is favorable due to its specific paramagnetic properties (high magnetic moment, long electron spin relaxation time) [15] and consequent large increase of a tissue image contrast. In order to reduce toxicity of metal ions and prevent their accumulation in body tissues, the metal ions must be applied in the form of highly stable complexes. Today, polyaminocarboxylates represent the most often studied and used complexing agents in molecular imaging. Among them, cyclen derivatives from DOTA (1,4,7,10-tetraazacyclododecane-1,4,7,10-tetraacetic acid) family exhibit excellent properties due to extremely high thermodynamic as well as kinetic stability of their complexes [9].

In the new generation of contrast agents, significant attention is paid to their biodistribution. Nowadays, a contrast agent is administered intravenously and displays a nonspecific distribution into tissues. In order to visualize specific tissues (e.g. cancer tissue, bones, etc.), biological markers with specific affinity for a particular tissue are attached to the molecules of contrast agents [16]. Such disease-specific contrast agents are called targeted contrast agents and the process itself targeting. Molecules of targeted contrast agent are capable of recognizing a specific moiety, which acts as early reporters of a certain pathology. Therefore, after administration the targeted contrast agent accumulates in the particular tissue and causes a local contrast enhancement. Using of the targeted contrast agents enables not only reduction of a necessary dose of a contrast agent (commonly used dose of the MRI contrast agent is up to 5 g for one examination) but also allows earlier diagnosis of certain disorders. The most often utilized targeting groups are peptides

A. Hamplová, et al.: *J. Sep. Sci.* 33 (2010) 658.

or polysaccharides, but also much simpler moieties such bisphosphonates were described [17 – 19].

Alzheimer's disease is a chronic neurodegenerative disorder that leads to progressive decline of cognitive functions including memory, decision-making, orientation to physical surroundings and language. Prior these symptoms occur, extracellular neurotic plaques containing the β -amyloid peptide can be found in a patient's brain. Early detection of the β -amyloid deposits *in vivo* is very difficult. It is caused mainly by limited permeability of a blood brain barrier for most of molecules including the compounds that are able to target β -amyloid deposits [20 – 21]. The development of markers of β -amyloid deposits in Alzheimer's disease has been a goal of researchers for several years [22]. Recently ^{11}C -radiolabeled small-molecules have been developed, capable of entering the brain and specifically targeting amyloid plaques for imaging with PET, such as several thioflavin T derivatives [23 – 24]. A major limitation of this method is the requirement for markers labelled with short-lived isotopes, such as ^{11}C with half-life of about 20 min.

In this work a targeting contrast agents for early recognition of Alzheimer's disease was in the centre of interest. MRI with suitable contrast agent would offer significant advantages for the diagnosis of Alzheimer's disease, such as optimal spatial resolution, harmless non-ionizing radiation and fast scans. Thus, the use of β -amyloid marker linked to a MRI contrast agent would constitute an attractive noninvasive *in vivo* imaging approach. Recently, Poduslo and co-workers have published utilizing of targeted contrast agent based on a certain peptide for imaging Alzheimer's disease plaques by MRI [25]. Nevertheless, due to its large size (molecular weight almost 5000 Daltons), several days or weeks of incubation with the contrast agent are necessary to obtain the labeling of amyloid plaques in transgenic mouse brain *in vivo*. A small molecule contrast agent (molecular weight under 1000 Daltons) should be an improvement because of faster target delivery and also easier synthesis, purification and characterization. One of the thioflavin T analogues, namely Pittsburgh compound B (PiB), was chosen for this purpose (for the structure see Figure 1). A PiB-derivative of DOTA was synthesized and further investigated.

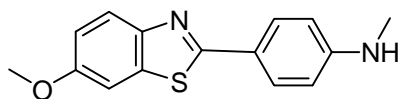


Figure 1. Pittsburgh compound B (PiB).

Synthesis of a MRI contrast agent is generally a multistep process with poor yields of a desired contrast agent. It is caused mainly by number of by-products of similar properties. Therefore many purifying steps are often necessary to obtain product of sufficient purity. The overall problem is monitoring of the reaction progress and characterization of reaction products, because typical methods like NMR, MS and TLC fail in case of certain polyaminocarboxylates. Therefore development of a versatile method preferably without special requirements for instrumentation is in the centre of interest.

For many steps during the synthetic procedures it is necessary to use the polyaminocarboxylate chelator in a protected form [26]. Furthermore, the protecting groups must be compatible with the low chemical stability of the biomolecules. These requirements are fulfilled with the *tert*-butyl ester group for protection of carboxylates. Therefore, many *tert*-butyl derivatives of DOTA-like ligands have been synthesized and studied. Among them, *t*Bu₃DO3A, i.e. 1,4,7,10-tetraazacyclododecan-1,4,7-tris(*tert*-butylacetate) is a crucial reaction intermediate widely used in the synthesis of ligands for molecular imaging (for the structure see Figure 3).

A lot of attention has been paid to the synthesis of DO3A (1,4,7,10-tetraazacyclododecane-1,4,7-triacetic acid) and its esterified forms as well. Despite this fact, an optimal synthetic procedure has not been reported yet. The synthetic strategy usually relies on alkylation of cyclen with corresponding halogen derivative (Figure 2). Beside the required DO3A ester, other products (esters of DOTA and DO2A, i.e. 1,4,7,10-tetraazacyclododecane-1,4-diacetic acid) are always present in the reaction mixture.

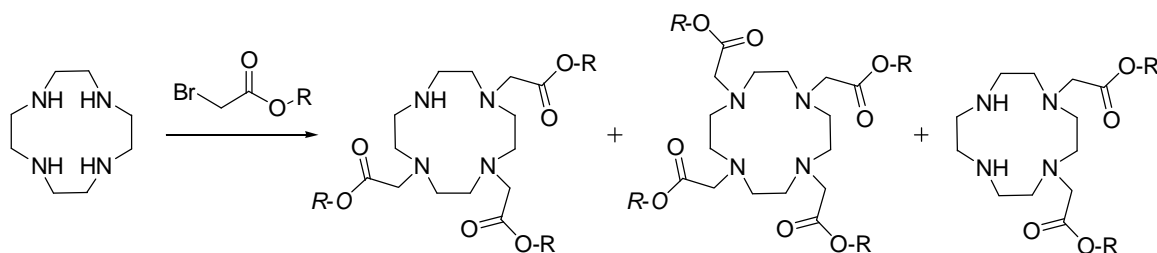


Figure 2. Scheme of the synthesis of esterified forms of DO3A.

Due to specific properties of different cyclen derivatives, separation and analysis of the reaction mixtures are highly problematic. Above all, one should mention their acid-base properties. Under all HPLC-suitable pH values, the *tert*-butyl esters of DOTA-like ligands contain two positively charged nitrogen atoms. Despite this fact, any of the studied *tert*-butyl esters is insoluble in pure water due to highly hydrophobic *tert*-butyl groups. Although an HPLC separation method has been reported within syntheses of several DOTA derivatives [27 – 30] and complexes [31 – 34], there is no systematic study in the literature providing reasonable methods for analysis of DO3A esters and by-products of their synthesis.

In this work, two separation techniques based on different principles, HPLC and CZE, were employed in development of the method suitable for analysis and quantification of different DOTA-like esters, i.e. *t*Bu₄DOTA, *t*Bu₃DO3A and *t*Bu₂DO2A (Figure 3). UV-VIS spectrometry was chosen for this purpose as the most common detection technique. This work is also the first case of a CZE application to the analysis of polyaminocarboxylates. Both methods can be considered as powerful tools for monitoring *t*Bu₃DO3A synthesis and the analysis of final products.

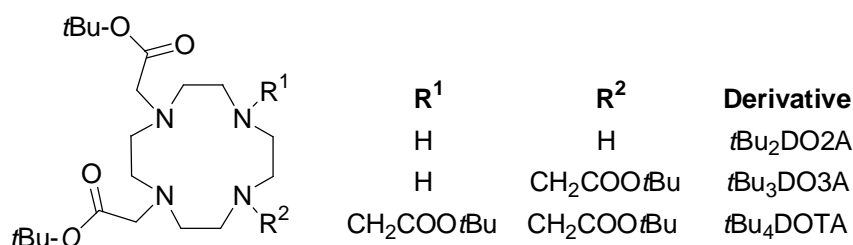


Figure 3. Structural formulas of the *tert*-butyl derivatives of DOTA-like ligands.

2.2 Experimental

2.2.1 Chemicals

Methanol (gradient grade purity) and acetonitrile (gradient grade purity) were purchased from Merck (Darmstadt, Germany). Triethylamine (purity 99.5%) was purchased from Fluka (Buchs, Switzerland). Trifluoroacetic acid, TFA (purity 99.9%) was supplied by Carl Roth (Karlsruhe, Germany). Ammonium acetate, thiourea and sodium hydroxide (all p.a. purity grade) were purchased from Penta (Prague, Czech Republic). Cyclen derivatives *t*Bu₄DOTA, i.e. 1,4,7,10-tetraazacyclododecan-1,4,7,10-tetrakis(*tert*-butylacetate), *t*Bu₃DO3A, i.e. 1,4,7,10-tetraazacyclododecan-1,4,7-tris(*tert*-butylacetate) and *t*Bu₂DO2A, i.e. 1,4,7,10-tetraazacyclododecan-1,4-bis(*tert*-butylacetate) were synthesized at the Department of Inorganic Chemistry, Faculty of Science, Charles University in Prague, Czech Republic using the synthetic procedure published elsewhere [35 – 37]. Water used in this work was purified with a Milli-Q water purification system (Millipore, USA).

2.2.2 Synthesis

Anisidine, *p*-nitrobenzoylchlorid, Lawesson reagent, *t*-butylbromoacetate and pyridine (all of synthetic purity) and K₃[Fe(CN)₆], NaHCO₃, P₂O₅, SnCl₂ (all p.a. purity) were purchased from Sigma Aldrich (Steinheim, Germany) and used as received. Acetonitrile was dried by distillation with P₂O₅. ¹H NMR and ¹³C NMR were recorded on a Bruker Avance DPX250 spectrometer (250.131 MHz) and a Bruker Avance II (400 MHz), in CDCl₃, DMSO or D₂O using 5mm sample tubes. Tetramethylsilane was used as an internal standard. Chemical shifts are given in ppm (δ -scale). Mass spectra were recorded on a Perkin–Elmer SCIEX AOI 300 spectrometer equipped with an electrospray ion source and an ion trap. All measurements were carried out in positive mode.

Synthesis of the PiB-DO3A

The targeting part of the ligand was prepared by modification of the procedure described in the original paper (Scheme 1, page 35) [38].

N-(4'-methoxyphenyl)-4-nitrobenzamide (2). A solution of 4-nitrobenzoyl chloride (2.2 g, 12 mmol) in toluene (15 ml) was added to a mixture of anisidine **1** (1.5 g, 12 mmol) and pyridine (2.9 ml, 36 mmol) in toluene (10 ml). The mixture was refluxed for 3 hours. After cooling to room temperature, the reaction was quenched with water. The precipitate was filtered under reduced pressure, washed with 5% aqueous solution of K_2CO_3 and water and dried on air at room temperature to give amide **2**. Yield: 2.1 g (61%) of yellow solid. Characterization corresponds to published data [38].

N-(4'-methoxyphenyl)-4-nitrothiobenzamide (3). Lawesson's reagent (1.8 g, 4.4 mmol) was added to a solution of **2** (2 g, 7.4 mmol) in chlorobenzene (5 ml). The reaction mixture was refluxed for 3.5 hours. The thioamide **3** precipitated out from the reaction mixture after cooling to room temperature and was filtered under reduced pressure and dried by passing air. Yield: 1.0 g (49%) of orange solid. Characterization corresponds to published data [38].

2-(4'-nitrophenyl)-6-methoxybenzothiazol (4). The thioamide **3** (0.5 g, 1.7 mmol) was wetted with ethanol and then 1.5 ml of 30% aqueous NaOH (0.6 g, 14 mmol) was added. The mixture was diluted with water (5 ml) to provide a final suspension of 10% aqueous NaOH. The mixture was slowly dropped into a stirred solution of $K_3[Fe(CN)_6]$ (2.3 g, 9.2 mmol) in water heated at 80 °C. The reaction mixture was heated for another 3 hours at 110 °C. The benzothiazol **4** precipitated out from the reaction mixture after cooling to room temperature and was filtered under reduced pressure, washed with water and dried on air at room temperature. Yield: 0.25 g (50%) of yellow-brown solid. Characterization corresponds to published data [38].

2-(4'-aminophenyl)-6-methoxybenzothiazol (5). $SnCl_2$ (4.7 g, 21 mmol) was added to a solution of benzothiazol **4** (1.0 g, 3.5 mmol) in ethanol (80 ml). The mixture was refluxed under argon atmosphere for 4 hours. Then ethanol was evaporated and the residue was dissolved in ethyl acetate (30 ml). The resulting solution was washed with 1M NaOH and water. The benzothiazol aminoderivative **5** was obtained after rotary evaporation. Yield: 0.7 g (80%) of brown solid. Characterization corresponds to published data [38].

Chloroacetamide (6). A suspension of K_2CO_3 (0.8 g, 6.0 mmol) in a solution of chloroacetyl chloride (0.35 g, 3.0 mmol) in dry acetonitrile (20 mL) was cooled to

0 °C. Then the solution of **5** (0.25 g, 1.0 mmol) in dry acetonitrile (30 mL) was slowly dropped into the suspension and the mixture was stirred overnight at room temperature. The mixture was filtered under reduced pressure. The solids were dissolved in chloroform (30 mL) and washed two times with water (2 x 20 mL). Pure product **6** was obtained after rotary evaporation of organic phase. Yield: 0.15 g (42%) of beige solid. ¹H NMR (CDCl₃, 250 MHz): δ 3.95 (s, 3 H, -OCH₃), 4.24 (s, 2 H, -CH₂Cl), 7.10 (d, 1 H, arom.), 7.36 (d, 1 H, arom.), 7.73 (d, 2 H, arom.), 7.95 (d, 1 H, arom.), 8.07 (d, 2 H, arom.), 8.36 (s, NH).

PiB-*t*Bu₃DO3A (7). A suspension of K₂CO₃ (0.2 g, 1.3 mmol) in a solution of *t*-Bu₃DO3A (0.2 g, 0.3 mmol) in dry acetonitrile (25 mL) was added to a suspension of **6** (0.1 g, 0.4 mmol) in dry acetonitrile (20 mL). The mixture was stirred for 48 hours at room temperature and then refluxed for 2 hours. After filtration and rotary evaporation of the filtrate, yellow oil **7** was obtained and used in a next step without further purification.

PiB-DO3A (8). The oil **7** was dissolved in a mixture of TFA (5 ml) and dry dichloromethane (5 ml) and heated at 45 °C overnight. After repeated evaporation with ethanol, the resulting solid was dissolved in 10 % aqueous ethanol (10 ml) and purified on a strongly acidic cation-exchange resin (Dowex 50, elution of impurities with 10% aqueous ethanol, elution of product with 5% NH₃ in 50% aqueous ethanol). After rotary evaporation, remaining NH₃ and the rest of organic impurities were removed on a weakly acidic cation-exchange resin (Amberlit CG50, elution of impurities with 50% aqueous ethanol, elution of product with 50% aqueous acetone). Yield: 0.1 g (40%) of white solid. ¹H NMR (D₂O): δ 3.71 (bs, 8H, macrocycle), 3.98 (bs, 8H, macrocycle), 4.08 (s, 4H, pendant), 4.28 (s, 3H, -CH₃), 4.37 (s, 4H, pendant), 7.34 (s, 2H, arom.), 7.93 (d, ³J_{H-H} = 7.65 Hz, 2H, arom.), 7.99 (s, 2H, arom.), 8.08 (d, ³J_{H-H} = 7.65 Hz, 1H, arom.).

Synthesis of *t*Bu₃DO3A (9)

t-Bu₃DO3A was prepared by modification of the reported procedure (Scheme 2, page 35) [37].

Cyclene (2.0 g, 11.6 mmol), NaHCO₃ (4.0 g, 47.7 mmol) and dry acetonitrile (70 mL) were mixed in a 250 mL round-bottom flask. The mixture was cooled at

0 °C and *t*-butylbromoacetate (7.0 g, 36.1 mmol) was added under stirring during 4 h. The mixture was stirred at room temperature overnight. The solids were filtered-off and the volatiles were removed by rotary evaporation. To the remaining solid, toluene (70 mL) was added and the suspension was stirred at room temperature overnight. The crude product was dissolved in dichloromethane (60 mL). Water (60 mL) was added and the mixture was vigorously stirred at room temperature overnight. The aqueous phase was removed and washed with dichloromethane (2 x 10 mL). The organic fractions were combined and dried with sodium sulfate. The solvent was partly evaporated to reach volume 30 mL. Then, hexane was added under stirring until fine cloud of the precipitate was formed and the mixture was left stand overnight. The solid was filtered, washed with hexane and dried by passage of air. The final product was obtained as a white powder. The yield was 3.1 g (45%). Characterization corresponds to published data [37].

2.2.3 HPLC instrumentation and conditions

The HPLC experiments were performed on an Ecom liquid chromatograph system (Prague, Czech Republic) comprising of a Beta 10 gradient pump, injection valve with a 10 μ L loop and an LCD 2084 absorbance detector. The system was equipped with an on-line degasser and a mixing chamber. The UV detection was carried out at wavelength of 200 nm. Analyses were performed on a LiChroCART Purospher STAR RP-18e column (150 \times 4.6 mm I.D., particle size 5 μ m) supplied by Merck (Darmstadt, Germany). A LiChroCART Purospher STAR RP-18e precolumn (4 \times 4.6 mm I.D., particle size 5 μ m) was used to prevent contamination of the analytical column. The chromatograms were recorded and evaluated through the CSW 1.6 software purchased from DataApex (Prague, Czech Republic).

The optimized mobile phase consisted of acetonitrile (A), aqueous solution of 0.1% trifluoroacetic acid (B) and water (C). A gradient elution program described in Table 1 with a flow rate of 0.8 mL/min was applied. For HPLC analysis, all samples were dissolved in acetonitrile/water mixture (30:70, v/v). All measurements were carried out at ambient temperature.

Table 1. The gradient elution program. Solvent A, pure acetonitrile; solvent B, 0.1% TFA in water; solvent C, pure water.

Time [min]	Solvent A [%]	Solvent B [%]	Solvent C [%]
0	30	25	45
10	75	25	0
15	75	25	0

2.2.4 CZE instrumentation and conditions

The CZE experiments were carried out on an Agilent 3D-CE instrument (Waldbronn, Germany). A fused silica capillary of 75 μm I.D., 80.0 cm total length and 71.5 cm effective length, was employed as the separation capillary. Hydrodynamic injection of samples was performed with an overpressure of 1.5 kPa for 20 seconds. The separation voltage was set to 30 kV. The capillary cassette temperature was maintained at 25 $^{\circ}\text{C}$. The diode array detector collected UV spectra within the range from 200 to 400 nm. The wavelength of 200 nm exhibited the highest sensitivity and was therefore chosen for the data evaluation. The electropherograms were processed using 3D-CE ChemStation software delivered by Agilent Technologies (Waldbronn, Germany).

The optimized background electrolyte (BGE) consisted of 20 mM ammonium acetate and 5 mM triethylamine, both dissolved in pure methanol ($\text{pH} \approx 8.8$, measured in water instead of methanol). The separation capillary was conditioned by flushing with 1 M NaOH for 20 minutes, followed by water for 10 minutes prior the first run each day. Between consecutive runs, the separation capillary was rinsed with BGE for 2 minutes. For CZE analyses, all samples were dissolved in methanol.

The inner wall of the separation capillary was negatively affected by the alkaline organic mixture of ammonium acetate and methanol used as the separation buffer and the solvent, respectively. Fused silica could dissolve in the BGE and thus, it was necessary to replace the separation capillary after every 50 measurements to ensure adequate repeatability. For the same reason, the separation capillary was

flushed with 1 M NaOH for 10 minutes, followed by water for another 5 minutes after each 10 analyses.

2.3 Results and discussion

2.3.1 HPLC method development

The acid-base properties of the studied compounds are similar to other derivatives of cyclen. Two amino groups show protonation constants in the basic region (pK 8 – 13), whereas the other two amino groups in the ring are protonated only under extremely acidic conditions ($pH < 0$). Hence, the compounds are present in mono- or di-protonated forms under the separation conditions used in HPLC. Applying various acetonitrile and methanol mixtures as the mobile phase, the analytes were eluted with retention times close to dead retention time. Moreover, despite using stationary phases with encapped silanol groups such as LiChrocart Purospher STAR RP-18e or LiChrosorb RP-Select B, the peak shape of the studied compounds was unsatisfactory. It means that ion character of the studied compounds caused by charged nitrogen atoms predominates over the hydrophobicity of the *tert*-butyl groups.

In such situation, addition of an ion-pair reagent can prove to be useful [39]. Every ion-pair reagent has an ionic end and a hydrophobic tail. A charged analyte is attracted to the oppositely charged functional group of an ion-pair reagent forming a neutral pair. The retention of analyte increases as a result of interaction between hydrophobic tail of ion-pair reagent and nonpolar stationary phase (as for example C18). To proof the applicability of the ion-pair reagent for this particular problem, the most common ion-pair reagent, i.e. octanesulphonic acid, was examined. The retention increased dramatically for all the studied *tert*-butyl esters of DOTA-like ligands. Unfortunately, utilizing octanesulphonic acid as an ion-pair reagent worsens the baseline noise and caused some ghost peaks. Not negligible was also UV absorbance of the octanesulphonic acid. Therefore alternative ion-pair reagents, i.e. phosphoric acid or TFA, were tested. Since both the acids do not contain a long hydrophobic chain, they are not typical ion-pair reagents. Nevertheless, in case of *tert*-butyl esters of DOTA-like ligands is much more important to suppress the

positively charged nitrogen atoms than enhance the hydrophobicity with ion-pair reagent's non-polar chain. Addition of phosphoric acid as well as TFA brings sufficient retention of all the studied analytes without significant deterioration of the baseline.

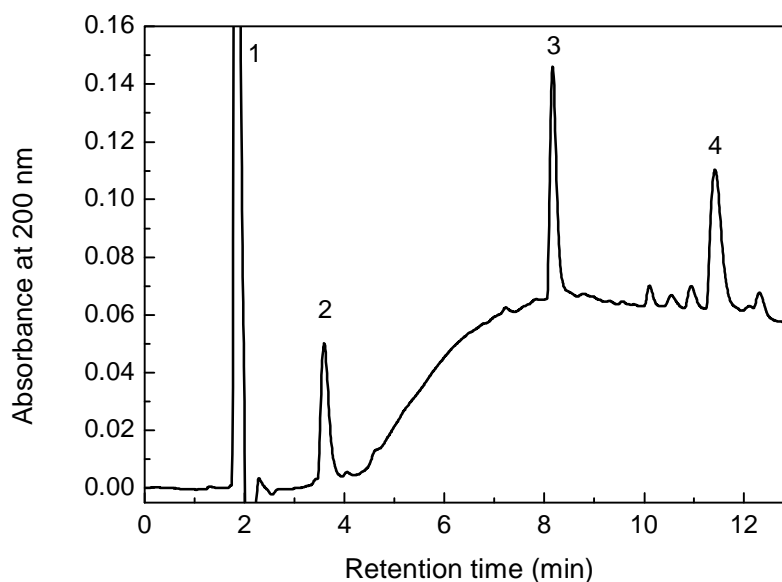


Figure 4. Chromatogram of the *tert*-butyl esters of DOTA-like derivatives (2.0×10^{-4} mol/L each) separated on a LiChroCART Purospher STAR RP-18e column using mobile phase gradient presented in Table 1. Detection wavelength $\lambda = 200$ nm. Peak identification: 1 – HBr, 2 – *t*Bu₂DO2A, 3 – *t*Bu₃DO3A, 4 – *t*Bu₄DOTA.

During the HPLC method optimization, the retention characteristics, the shape of peaks and time of analysis were in the centre of the interest. Besides the above mentioned characteristics, the absorbance of each mobile phase component was also taken into account due to necessity of detection at extremely low wavelength (200 nm). The best results were obtained with the mobile phase containing 0.1% TFA as an ion-pair reagent and acetonitrile as an organic modifier. The preliminary experiments [40] have shown that the difference in hydrophobicity of the three *tert*-butyl DOTA derivatives is too large for using a simple isocratic

elution and that is why the gradient elution was employed. The optimized gradient program, see Table 1, offers a rapid and simple separation method. All the peaks were highly symmetric and baseline resolved with analysis times lower than 12 minutes (Figure 4). The small peaks that eluted with retention times between 10 and 12 minutes correspond to impurities present in the samples of the studied compounds. However, it is evident that the optimized HPLC method provides a satisfactory resolution between the compounds of interest and accompanying impurities. Increasing amount of acetonitrile in the mobile phase during the gradient elution program caused the baseline drift. The first peak in the chromatogram corresponds to hydrobromide (HBr), which was proven by spiking the analysed sample with a pure HBr. The presence of HBr in all the studied *tert*-butyl DOTA-like derivatives is given by the procedure of their preparation, because they are synthesized as hydrobromides.

2.3.2 CZE method development

Due to the poor solubility of the investigated compounds in water, pure methanol was chosen as the BGE solvent to realize non-aqueous CZE. Various buffering salts, easily soluble in methanol, were tested for preparation of the BGE within the pH range 4.0 – 9.5. The BGEs of higher pH values were prepared by addition of triethylamine (TEA). The best results were obtained with the BGE in basic region. On the other hand, increasing concentration of TEA prolonged the analysis time and worsened the peak shape. The optimized BGE contained 20 mM ammonium acetate and 5 mM triethylamine (pH = 8.8, measured in water instead of methanol) and yielded an electropherogram depicted in Figure 5. It is evident that these experimental conditions offer a fast separation of all three investigated compounds with the migration times shorter than 11 minutes. The peaks of *t*Bu₄DOTA and *t*Bu₃DO₃A were perfectly symmetrical with the height equivalent to a theoretical plate (HETP) of 5.3 μ m and 8.0 μ m, respectively. On the contrary, the *t*Bu₂DO₂A peak was much broader with HEPT of 16.1 μ m, which could be explained by different acid-base behaviour. The inner wall of the capillary was negatively affected by the combination of the alkaline separation buffer and

methanol. Thus, it was necessary to wash the capillary with NaOH solution regularly or replace it as stated in the Experimental section (page 23).

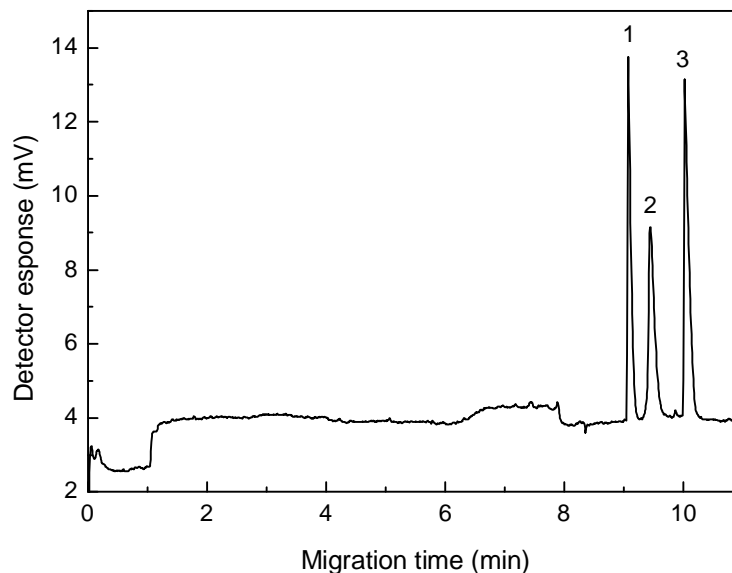


Figure 5. Electropherogram of the *tert*-butyl esters of DOTA like derivatives (5.0×10^{-4} mol/L each) separated by CZE in the BGE of 20 mM ammonium acetate and 5 mM triethylamine dissolved in methanol (pH = 8.8). Peak identification: 1 – Bu₃DO3A, 2 – *t*Bu₂DO2A, 3 – *t*Bu₄DOTA.

2.3.3 Quantification

Calibration curves within the concentration interval of 1.0×10^{-5} to 1.0×10^{-3} mol/L for all the three *tert*-butyl esters of DOTA-like ligands were measured in HPLC and CZE under the optimized separation conditions described above. Due to a non-optimal peak shape, which has been discussed in the previous paragraph, the calibration curve for *t*Bu₂DO2A in CZE was studied within a limited concentration interval of 2.0×10^{-5} to 1.0×10^{-3} mol/L. The measurements at all concentrations were carried out in triplicate and the mean peak areas were plotted against the analyte concentration and subjected to linear regression to obtain individual parameters of the calibration lines expressed by the equation (1)

$$A = a + b \times c^i \quad (1)$$

where A is the mean peak area, a is the intercept, b is the slope and i is the linearity factor. The parameters of the calibration curves, the correlation coefficients and the limits of detection (LOD) and quantification (LOQ) from HPLC and CZE are summarized in Table 2 and 3, respectively. The correlation coefficients perfectly limit to 1.000 for all the calibration curves in both separation methods. None of the intercepts of the calibration lines were found to be significantly different from zero at the significance level of $\alpha = 0.05$ applying the t -test for intercepts (i.e. $t = a/SD_a$; SD_a is a standard deviation for a) [41].

Consequently, the linearity of the calibration curves was investigated by regression analysis in logarithmic coordinates using the equation (2)

$$\log A = \log \beta + i \times \log c \quad (2)$$

Data obtained by the logarithmic regression, i.e. the linearity factor (i) and the logarithm of slopes ($\log \beta$), are compared (Table 4) with the logarithm of slopes ($\log b$) calculated from data in Table 2 and 3. There is a perfect agreement between the logarithmic slopes calculated from both regression analyses, i.e. $\log \beta$ and $\log b$. That confirms again that the intercepts are statistically insignificant from zero. All the linearity factors are very close to 1.00 and therefore the peak areas are directly proportional to the molar concentration of all the studied derivatives. Excellent linearity of the calibration curves were noticed within the concentration interval of 1.0×10^{-5} to 1.0×10^{-3} mol/L for all the studied compounds except for $t\text{Bu}_2\text{DO}_2\text{A}$ in CZE analysis. As an example, HPLC and CZE calibration curves and logarithmic regression curves for $t\text{Bu}_4\text{DOTA}$ are shown in Figures 6 and 7, respectively.

Table 2. Parameters of the calibration curves obtained in HPLC with standard deviations (SD) in parentheses. Slope, b ; intercept, a ; correlation coefficient, r ; limit of detection, LOD and limit of quantification, LOQ.

Derivative	b (SD) [V.s.L/mol]	a (SD) [V.s]	r	LOD [mol/L]	LOQ [mol/L]
t Bu ₄ DOTA	3790 (34)	-0.035 (0.026)	0.9994	3.3×10^{-6}	3.6×10^{-5}
t Bu ₃ DO3A	3480 (21)	0.026 (0.016)	0.9997	3.4×10^{-6}	3.9×10^{-5}
t Bu ₂ DO2A	2500 (16)	-0.004 (0.012)	0.9997	5.6×10^{-6}	2.0×10^{-5}

Table 3. Parameters of the calibration curves measured in CZE with standard deviations (SD) in parentheses. Slope, b ; intercept, a ; correlation coefficient, r ; limit of detection, LOD and limit of quantification, LOQ.

Derivative	b (SD) [V.s.L/mol]	a (SD) [10^{-3} .V.s]	r	LOD [mol/L]	LOQ [mol/L]
t Bu ₄ DOTA	74.6 (0.4)	-0.032 (0.243)	0.9997	5.9×10^{-6}	1.7×10^{-5}
t Bu ₃ DO3A	98.9 (0.7)	-0.633 (0.448)	0.9996	1.2×10^{-5}	2.4×10^{-5}
t Bu ₂ DO2A	74.3 (1.9)	-0.772 (0.188)	0.9993	2.4×10^{-5}	8.7×10^{-5}

Table 4. Parameters of the calibration curves plotted in the logarithmic coordinates. Linearity factor, i ; logarithm of slope from the equation (2), $\log \beta$; logarithm of slope from the equation (1), $\log b$.

Method	HPLC			CZE		
	i	$\log \beta$	$\log b$	i	$\log \beta$	$\log b$
<i>t</i> Bu ₄ DOTA	0.97	6.453	6.578	0.98	4.739	4.873
<i>t</i> Bu ₃ DO3A	0.94	6.327	6.540	1.05	5.154	4.995
<i>t</i> Bu ₂ DO2A	0.99	6.367	6.398	1.09	5.161	4.850

Both methods were also compared in terms of their repeatability. A sample containing 1.0×10^{-3} mol/L of each DOTA derivative was analyzed ten times in a row and the mean values (\bar{x}), standard deviations (SD) and relative standard deviations (RSD) of peak area (A), peak height (h) and retention/migration time (t) were calculated. The results are summarized in Tables 5. The HPLC method provides an outstanding repeatability for all studied compounds and is markedly more robust than CZE. The day-to-day repeatability of the HPLC method was almost as good as the run-to-run one. However, the day-to-day repeatability of the CZE analysis was strongly influenced by the problem of dissolving fused silica in the BGE as already discussed above.

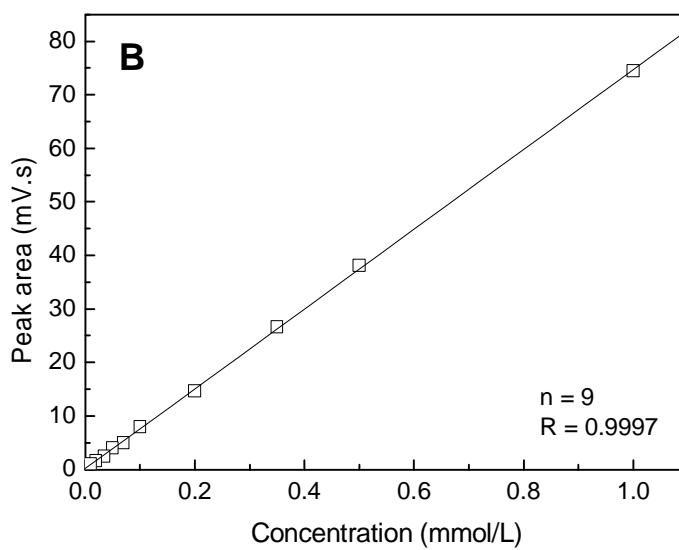
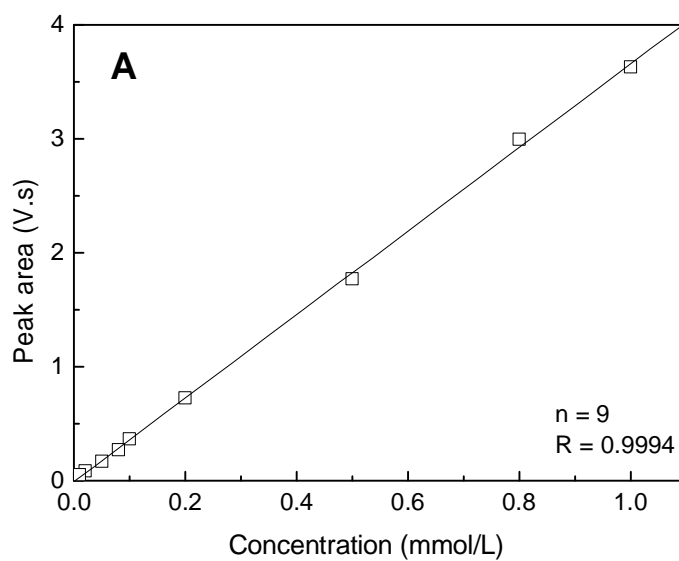


Figure 6. Calibration curves (peak area vs. concentration) for *t*Bu₄DOTA within a concentration interval of 1.0×10^{-5} to 1.0×10^{-3} mol/L measured by the optimized HPLC (A) and CZE (B) methods.

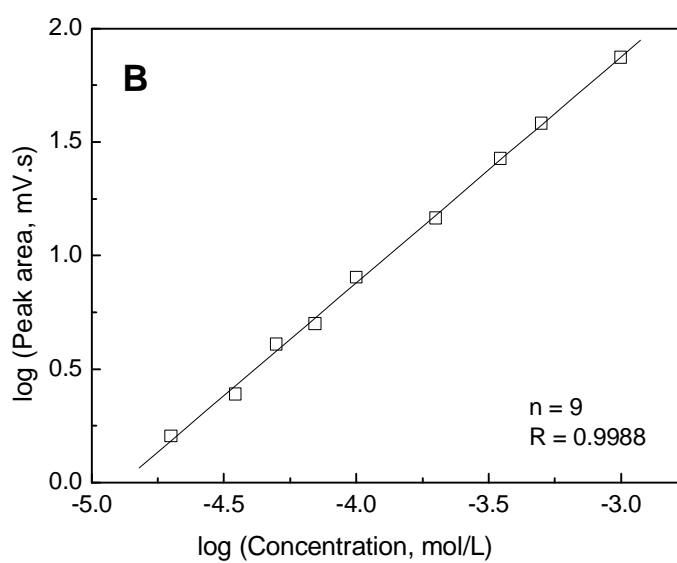
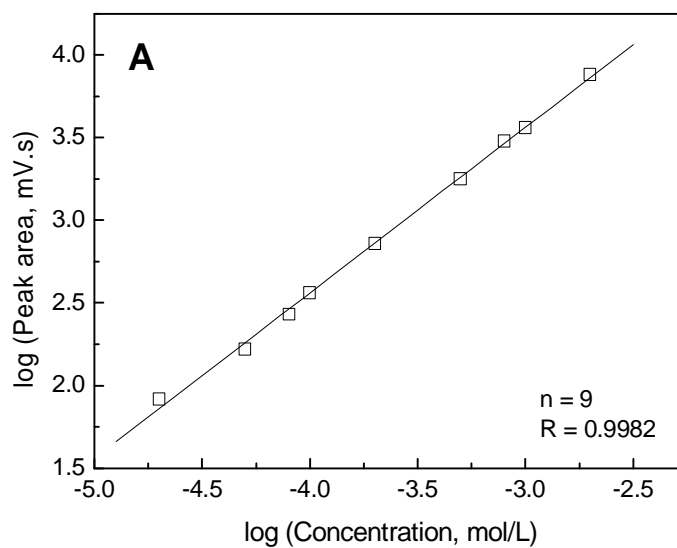


Figure 7. Dependence of logarithm of the peak area on logarithm of the *t*Bu₄DOTA concentration in the linear range of 2.0×10^{-5} to 2.0×10^{-3} mol/L obtained by the optimized HPLC (A) and CZE (B) methods.

Table 5. The repeatability of the optimized HPLC and CZE methods measured on the sample containing 1.0×10^{-3} mol/L of each DOTA derivative. Retention/migration time, t_R/t_{mig} [min]; peak area, A [$mV \cdot s$], peak height, h [mV].

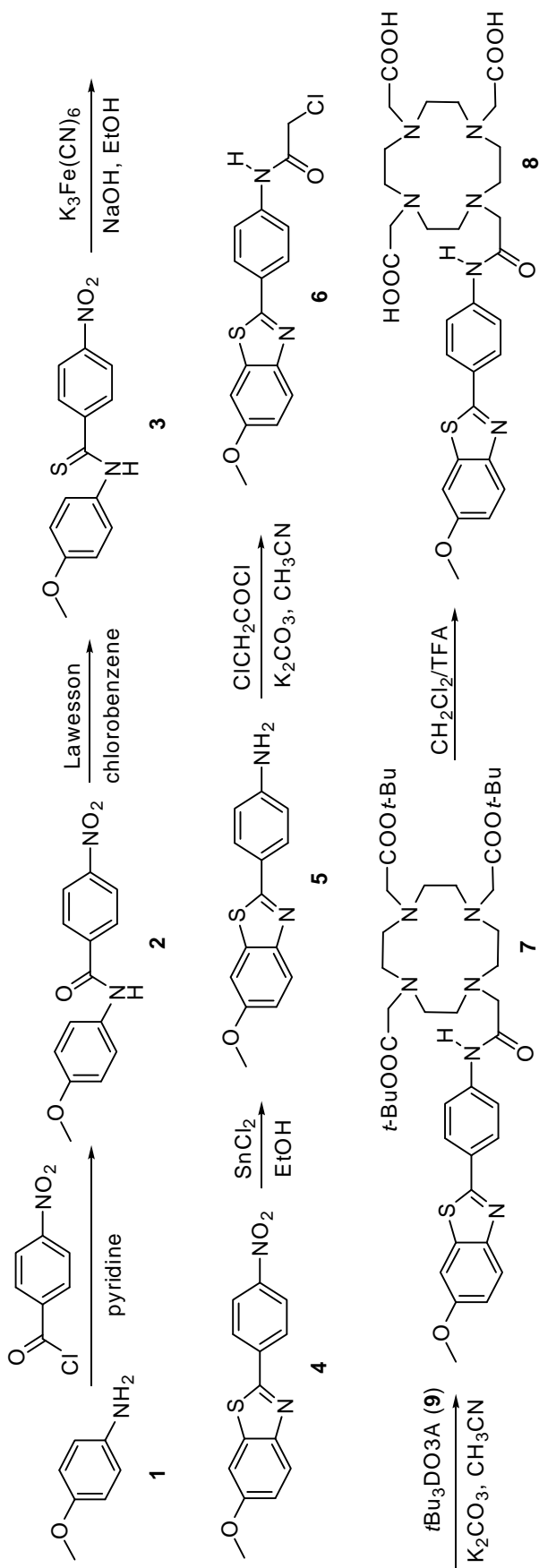
Derivative	tBu_4DOTA			tBu_3DO3A			tBu_2DO2A		
	t_R/t_{mig}	A	h	t_R/t_{mig}	A	h	t_R/t_{mig}	A	h
HPLC	\bar{x}	3581	147.3	7.95	3525	239.4	3.25	2534	152.8
	SD	80	3.6	0.02	81	4.5	0.04	70	4.1
	RSD%	2.2	2.4	0.2	2.3	1.9	1.2	2.8	2.7
CZE	\bar{x}	130.2	21.25	10.04	97.1	13.61	9.43	94.9	10.33
	SD	7.4	1.29	0.07	5.3	0.56	0.10	5.68	0.48
	RSD%	5.7	6.1	0.7	5.5	4.1	1.1	6.0	4.6

2.3.4 Applications in the syntheses of *t*Bu₃DO3A and PiB-*t*Bu₃DO3A

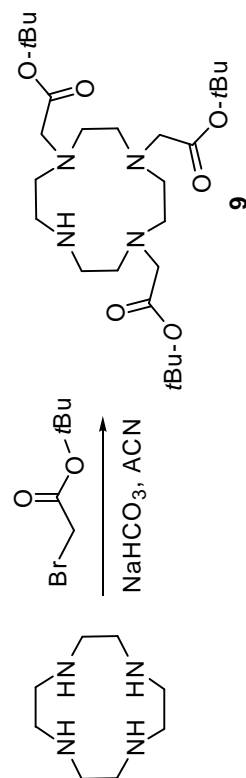
The optimized HPLC and CZE methods were used for monitoring of the reaction progress during the synthesis of the novel targeted contrast agent PiB-DO3A. Firstly, the targeted part **5** was prepared by modification of the procedure described in the original paper (Scheme 1) [38]. The reaction sequence starts with a reaction of anisidine **1** with *p*-nitrobenzoyl chloride, which yields the amide **2**. Treatment with the Lawessons reagent gives the thioamide **3** that undergoes the cyclization by action of K₃[Fe(CN)₆]. The final aminoderivative of thioflavine **5** was obtained by reduction of **4** with SnCl₂. Whole this part of the synthesis was monitored by ¹H NMR without any problem.

The macrocyclic chelate *t*-Bu₃DO3A (**9**) was prepared by an alkylation of cyclen with *t*-butylbromoacetate (Scheme 2). Finally, the targeted part **5** was conjugated with *t*Bu₃DO3A using chloroacetyl chloride. Monitoring of the reaction progress in this part of the synthesis appeared as a serious problem. The purity of organic compounds is often followed by sophisticated methods like NMR, either ¹H or ¹³C, and MS. The progress of synthesis can also be examined by TLC, which represents quite simple but not very sensitive method with limited selectivity. Presence of a cyclic polyamine with the *tert*-butyl groups in reaction mixture brings certain difficulties into the monitoring of the synthesis and purity control of the final products. For example ¹H NMR, which is very powerful technique for identification of many other compounds, absolutely fails in case of cyclic polyamines due to slow dynamics of the molecular motion in aqueous solution. Such behaviour of cyclic polyamines results in broad signals that cannot be evaluated properly and therefore cannot be used for monitoring of the reaction progress. Other possibility represents MS, which could answer the question, if the desired compound is presented in a sample but without precise quantification.

Therefore development of a versatile method for analyzes of the *tert*-butyl esters of cyclen derivatives was in the centre of interest. Two methods using common separation instrumentation, HPLC and CZE with UV detection, were developed for this purpose and practically tested in the synthesis of a new targeted contrast agent.



Scheme 1. Synthesis of the ligand PiB-DO3A.



Scheme 2. Synthesis of *t*Bu₃DO3A.

Monitoring of the *t*Bu₃DO3A synthesis

The optimized HPLC and CZE methods were used for a *t*Bu₃DO3A synthesis monitoring. Samples of a real reaction mixture were taken during the synthesis. The mixture was filtered in order to get rid of solids containing inorganic salts and without any further pretreatment analyzed. It was found out that both methods are readily applicable for the *tert*-butyl esters determination. In spite of the fact that sample was dissolved in acetonitrile, there were no problems observed during CZE analysis. Results of the both methods were fully comparable (see Figures 8 and 9). The tested mixture contained 95% of *t*Bu₃DO3A with only 5% *t*Bu₄DOTA and no *t*Bu₂DO2A. There is a peak of an impurity in the chromatogram very close to the *t*Bu₃DO3A peak, which could lower precision of peak area determination and consequently worsen the reliability of the HPLC analysis. Therefore the optimized CZE method could be considered more suitable for analyzing of a real reaction mixture due to less interfering peaks in the electropherogram.

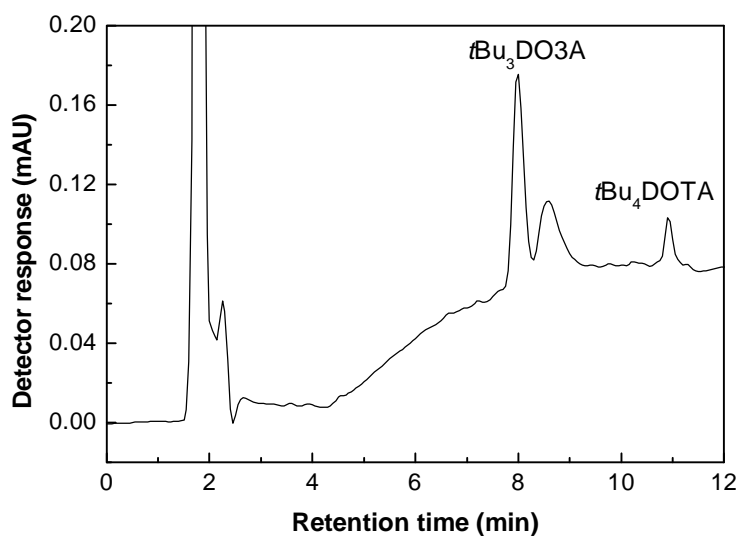


Figure 8. The optimized HPLC analyses of the real reaction mixture containing *t*Bu₃DO3A and *t*Bu₄DOTA. Conditions: Purospher STAR RP-18e column, mobile phase gradient presented in Table 1 (page 23), detection at $\lambda = 200$ nm.

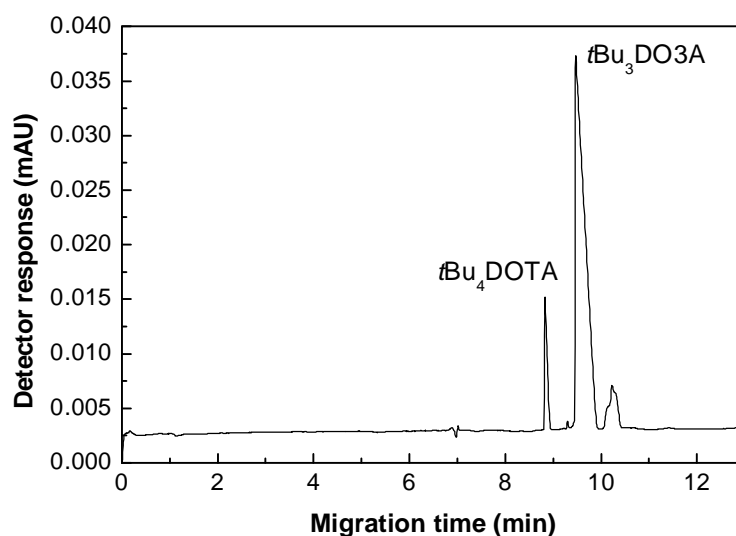


Figure 9. The optimized CZE analyses of the real reaction mixture containing $t\text{Bu}_3\text{DO3A}$ and $t\text{Bu}_4\text{DOTA}$. Conditions: BGE consisted of 20 mM ammonium acetate and 5 mM triethylamine dissolved in methanol (pH = 8.8), hydrodynamic injection (1,5 kPa, 20 s), detection at $\lambda = 200$ nm.

Analysis of PiB- $t\text{Bu}_3\text{DO3A}$

The optimized CZE method was successfully employed during the synthesis of targeted MRI contrast agent PiB-DO3A. The goal was determination of the amount of unreacted $t\text{Bu}_3\text{DO3A}$ in a sample of PiB- $t\text{Bu}_3\text{DO3A}$. Although the CZE method was not optimized for PiB- $t\text{Bu}_3\text{DO3A}$ analysis, the same conditions were used as in case of $t\text{Bu}_3\text{DO3A}$ reaction mixture. Since the crude PiB- $t\text{Bu}_3\text{DO3A}$ is yellow-brown oil, a filtration step was skipped. The oil was dissolved in methanol directly and used for the analysis. The resulted electropherogram is depicted in Figure 10. Longer migration time of PiB- $t\text{Bu}_3\text{DO3A}$ ($t_{\text{mig}} = 26.4$ min) than migration time of $t\text{Bu}_3\text{DO3A}$ ($t_{\text{mig}} = 8.8$ min) is probably caused by larger molecule of PiB- $t\text{Bu}_3\text{DO3A}$ when compared to $t\text{Bu}_3\text{DO3A}$. Although the analysis time increased, the resulted peaks were narrow and symmetrical. Presence of $t\text{Bu}_3\text{DO3A}$ in a reaction mixture documents incomplete conversion of the starting material. The CZE analysis of the

reaction mixture would enable further optimization of PiB-*t*Bu₃DO3A synthesis, especially reaction time and temperature needed for a higher conversion.

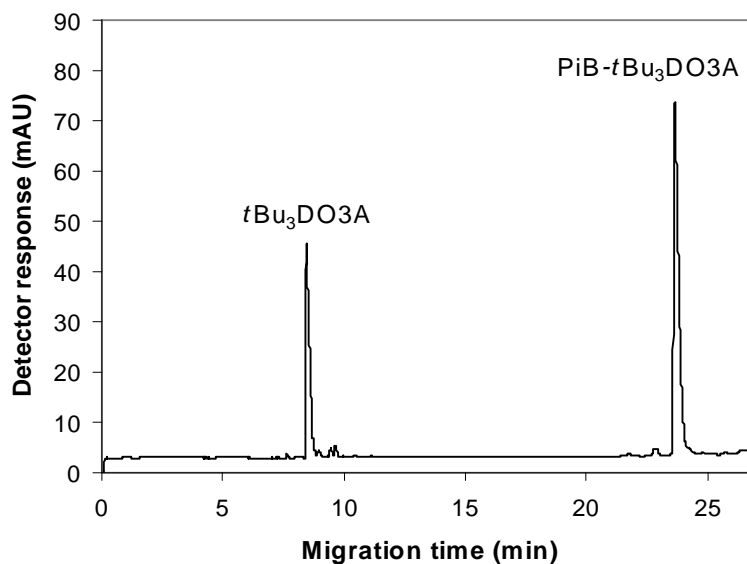


Figure 10. The optimized CZE analysis of the crude PiB- *t*Bu₃DO3A. Conditions: BGE consisted of 20 mM ammonium acetate and 5 mM triethylamine dissolved in methanol (pH = 8.8), hydrodynamic injection (1.5 kPa, 20 s), detection at $\lambda = 200$ nm.

2.4 Conclusion

To sum up, three DOTA-like derivatives, i.e *t*Bu₄DOTA, *t*Bu₃DO3A and *t*Bu₂DO2A, which are important reaction intermediates in the synthesis of contrast agents for molecular imaging, were studied by HPLC and CZE. The optimized HPLC method applies gradient elution of acetonitrile and water with 0.1% TFA to the LiChroCART Purospher STAR RP-18e column and the optimized non-aqueous CZE method uses 20 mM ammonium acetate and 5 mM triethylamine in pure methanol. The developed methods provide determination of the studied compounds with short analysis times, less than 12 minutes for both techniques. Both methods show satisfactory efficiencies, good repeatability and the LOD and LOQ values on the concentration level of 10^{-6} mol/L and 10^{-5} mol/L, respectively.

Use of the optimized HPLC and CZE methods for analysis of a real reaction mixture obtained by preparation of *t*Bu₃DO3A has shown a full applicability of the developed methods. Moreover, no sample pretreatment has been necessary. When comparing both optimized methods, HPLC offers more repeatable analysis with slightly higher sensitivity expressed by lower LOD and LOQ than those in CZE. On the other hand, CZE provides analyses with less interfering peaks and lower consumption of a sample.

The optimized CZE method was also employed in analysis of a reaction mixture during a synthesis of the novel targeting contrast agent PiB-DO3A. The conversion in the crucial reaction step, i.e. conjugation of the targeting part with *t*Bu₃DO3A, was followed by the CZE method without any pretreatment.

3 SOLID-PHASE DERIVATIZATION IN HPLC

3.1 Introduction

3.1.1 Derivatization in HPLC

Every separation technique, including HPLC, is incomplete without a suitable method of detection. The most widely used detection technique, UV-VIS spectrometry, became a standard equipment of any chemical laboratory. The biggest advantage of UV-VIS spectrometry is its versatility and economically undemanding operation. On the other hand, UV-VIS detection is applicable only for analytes containing a chromophore group in their molecule like for example aromatic ring, conjugated double bonds, etc. Detection of compounds lacking a UV-VIS absorbing moiety is usually carried out by an expensive and/or not very common instrumentation like mass spectrometry (MS), tandem mass spectrometry (MS/MS), evaporative light scattering detector (ELSD), refractive index detector (RID), conductivity detector (CD), fluorometric detection (LIF), chemiluminescent detector (CLD), inductively coupled plasma atomic emission spectroscopy (ICP-EAS), nuclear magnetic resonance (NMR) or by electrochemical detection (ECD) [42 – 45]. None of these techniques could be considered superior to all the others and free of drawbacks.

Another possibility represents derivatization [46]. During the derivatization step a UV-VIS non-responding analyte can be converted into a compound with significant absorbance. That allows determination with a higher sensitivity. For the derivatization reaction there are two common alternatives – pre-column derivatization, where the derivatization step takes place before the separation itself, and post-column derivatization, where the derivatization is realized between a separation column and a detector.

Both pre-column and post-column derivatization could be realized off-line or on-line. In the off-line mode of derivatization, the treatment with derivatization agent occurs out of the separation system. In the on-line arrangement of derivatization, the

A. Kubíčková, et al.: *J. Sep. Sci.* 34 (2011), DOI 10.1002/jssc.201100561.

reaction with derivatization agent is fully integrated into the separation system (Figure 11). The off-line mode is less common, because it is time consuming and brings a risk of sample contamination during a manipulation. However, there are some analyses where off-line derivatization is absolutely irreplaceable. Typically it could enhance detection limit in case of very low concentration of analyte in a complex matrix [47]. Another application of off-line derivatization is the derivatization of large molecules, where kinetics is the limiting factor.

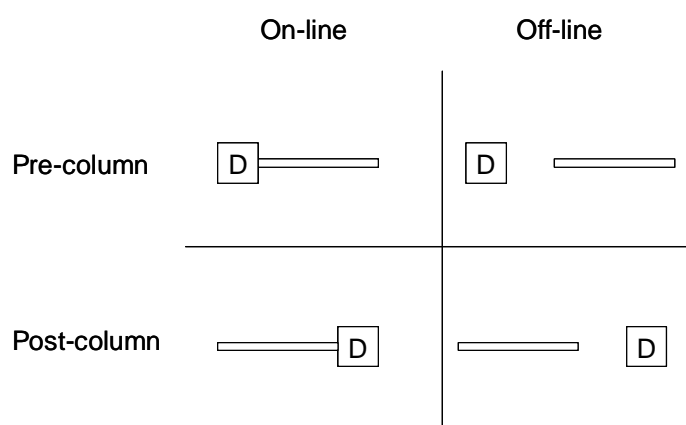


Figure 11. Scheme of the possible derivatization modes.

Generally, the predominant set-up in HPLC analyses is on-line derivatization regardless of pre- or post-column execution. Usually it is carried out by inserting a secondary fluid delivery system into the HPLC system. The main drawback of the on-line derivatization is superfluous increase of the void volume, decrease in the separation efficiency, sample dilution, sometimes larger baseline noise and last but not least longer analysis time. Another limitation could be the requirement for the compatibility of the mobile phase with the derivatization agent.

The disadvantages of the homogenous derivatization could be overcome by using a solid-state reactor [46, 48 – 51]. Solid-state reactors represent not very common, but very neat form of the on-line derivatization. The reactors can be used either prior the separation or in post-column mode. Basically, they are composed of immobilized derivatization agent in a matrix such as styren-divinylbenzene copolymer, silica or alumina. The active reagent can be either adsorbed or ionically

and/or covalently bond to a matrix. Moreover they bring the advantage of having no special requirements for the mobile phase and no excess use of a derivatization agent.

3.1.2 Amino acids

From the chemical point of view, an amino acid is considered every compound, which contains both amine and carboxylic group. There are thousands of compounds that meet this definition. Among them, α -amino acids i.e. those amino acids with amine group bonded to the carbon atom adjacent to the carboxylic group are of special importance because they include 20 proteinogenic amino acids. Their chemical properties emerge from the two functional groups as well as from the side chain. Due to the presence of a basic amine group and an acidic carboxylic group amino acids form internal salts sometimes called zwitterions. That is why behaviour of amino acids is strongly pH dependent. The side chain can be either aliphatic or aromatic or even contain other polar functional group. Based on the structure of the side chain, proteinogenic amino acids are divided into four main groups: neutral hydrophilic (Gly, Ser, Thr, Pro, Cys, Asn, Gln), neutral hydrophobic (Ala, Val, Leu, Ile, Phe, Tyr, Trp, Met), acidic amino acids (Glu, Asp) and basic amino acids (His, Lys, Arg).

Analysis of amino acids belongs among the topics that are solved most frequently not only in current analytical chemistry, but also in industry and clinical facilities. Numerous publications (70,000 published papers in the last ten years) dealing with this topic provide clear evidence. In the first half of 20th century, amino acids were studied by classical analytical methods (colorimetry, conductometric titration, paper chromatography, etc.) or enzymatic methods. The first automated amino acid analyzer based on ion-exchange chromatography with UV-VIS detection after derivatization with ninhydrin was introduced in 1951 by Moore and coworkers. Nowadays, nobody can imagine their analysis without suitable instrumentation. The prevailing techniques in amino acids determination are HPLC [52 – 55] and CZE [56 – 59]. The drawback of a CZE separation of amino acids is their interaction with free silanols on the surface of a bare fused-silica capillary. However, this problem could be overcome by using coated silica capillary or by putting specific

additives into the background electrolyte [60 – 62]. There are also less common methods successfully used for the separation and analysis of amino acids like for example micellar electrokinetic chromatography (MEKC) [63], capillary gel electrophoresis (CGE) [64], capillary liquid chromatography (CLC) [65] and capillary electro-chromatography (CEC) [66]. Even though amino acids are not readily volatile compounds, gas chromatography (GC) was also employed in their analysis. To transform them into a volatile form, many different derivatization procedures were utilized. The derivatization is mostly based on transformation of the carboxylic group into ester by reaction with an alcohol (for example isopropylalcohol) and subsequently acylation of an amino group by an anhydrid (for example trifluoroacetanhydrid) [67]. Chloroformates are widely used derivatization agents, because they react with both amino and carboxylic group and the derivatization is carried out in one single step [68].

This work is focused on the firstly mentioned instrumentation method, i.e. HPLC. Numerous publications cover the topic of HPLC separation of amino acids [52 – 55]. The prevalent problem remains detection. In spite of the fact that during the last years MS became almost standard equipment in analytical laboratories, the most widely used detection technique is still UV-VIS spectrometry. For most of amino acids it provides low sensitivity due to the lack of strong chromophore in their molecules. However, direct UV detection at wavelength of 190 – 214 nm may be employed [69 – 70]. Such detection suffers from low sensitivity and precision caused by negative effects typical for short wavelengths, such as system peaks, solvent effects or significant absorbance of trace impurities. In order to improve sensitivity of detection, a great variety of derivatization agents have been prepared and studied in detail. The most commonly used are the following: *o*-phthalaldehyd (OPA), phenylisothiocyanate (PITC), (5-dimethylamino)naphthalene-1-sulphonyl chloride (dansyl), 9-fluorenylmethylchloroformate (FMOC), 6-aminoquinolyl-*N*-hydroxy-succinimidyl carbamate (AQC) and ninhydrin [71 – 76]. For the structures see Figure 12. All these derivative reagents, except for PITC and ninhydrin, form with amino acids products detectable either by UV-VIS or fluorescence detection. Generally, fluorescence detection is less common, more expensive but also more sensitive than

UV-VIS detection. For typical time of derivatization and detection wavelength of each derivatization agent see Table 6.

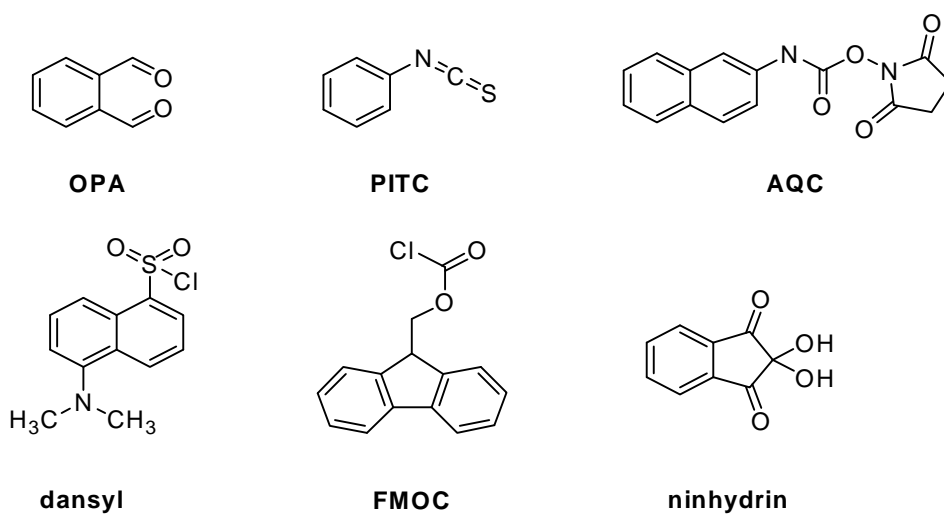


Figure 12. Structures of derivatization agents commonly used for amino acids derivatization.

Table 6. Typical detection wavelength and other characteristics of the derivatization agents.

Reagent	Type of derivatization	Time of derivatization (min)	Detection technique	Wavelength (nm)	Ref.
OPA	Pre- and postcolumn	15 – 30	UV	338	75, 77
			Fluorescence	337/454	
PITC	Precolumn	10 – 20	UV	254	72, 78
FMOc	Precolumn	20 – 30	UV	262	73, 79
			Fluorescence	254/313	
Dansyl	Pre- and postcolumn	35 – 60	UV	254	80, 81
			Fluorescence	365/510	
AQC	Precolumn	10	UV	248	74, 82
			Fluorescence	250/395	
Ninhydrin	Postcolumn	10	UV	570	76, 83

Besides these derivatizations, which are based on formation of covalent bonds, complexation with a transition metal and consecutive UV-VIS/fluorescence detection were utilized. This derivatization uses the well-known fact that amino acids are able to form stable complexes with certain metals, for example copper, quite quickly. Copper(II) complexes of amino acids show significant absorbance in the UV region (220 nm to 240 nm) due to intensive charge-transfer bands and also weaker absorbance in visible region due to d-d transitions. This property of the Cu(II) complexes is utilized for sensitive detection by UV-VIS spectrometry. Solution of transition metal cation, in most cases Cu(II), was delivered to analytes prior the separation or directly during the separation as a part of the mobile phase [84 – 85]. Despite this set-up of derivatization provided promising results, it has never become widely used.

In this work a new approach was applied to the amino acid derivatization. A solid-state reactor based on copper(II) oxide was developed and firstly introduced into HPLC system with UV-VIS detection. Such arrangement was tested on amino acids and other nitrogen-containing compounds. The main criterion was detection sensitivity increase, but influence of a mobile phase pH, applied flow-rate and stability of the reactor during analyses were also in center of the interest.

3.1.3 Applicability study

Linear and cyclic polyamines represent a group of compounds of many interesting properties. Above all, one should mention their chelating potential given by presence of lone electron pair at every nitrogen atom. Most of the applications are based on this ability to form complexes easily. Here are just few examples of polyamines applications: chemical catalysis, pharmaceuticals (MRI contrast agents, radiopharmaceuticals, luminescence probes), detoxification, etc.

Number of amino groups in the molecule as well as the sterical arrangement has a principle influence on their coordination properties, especially stability of a complex, rate of complex formation, selectivity for a particular metal ion, etc. The complexation properties of polyamines were described in numerous publications [86 – 88].

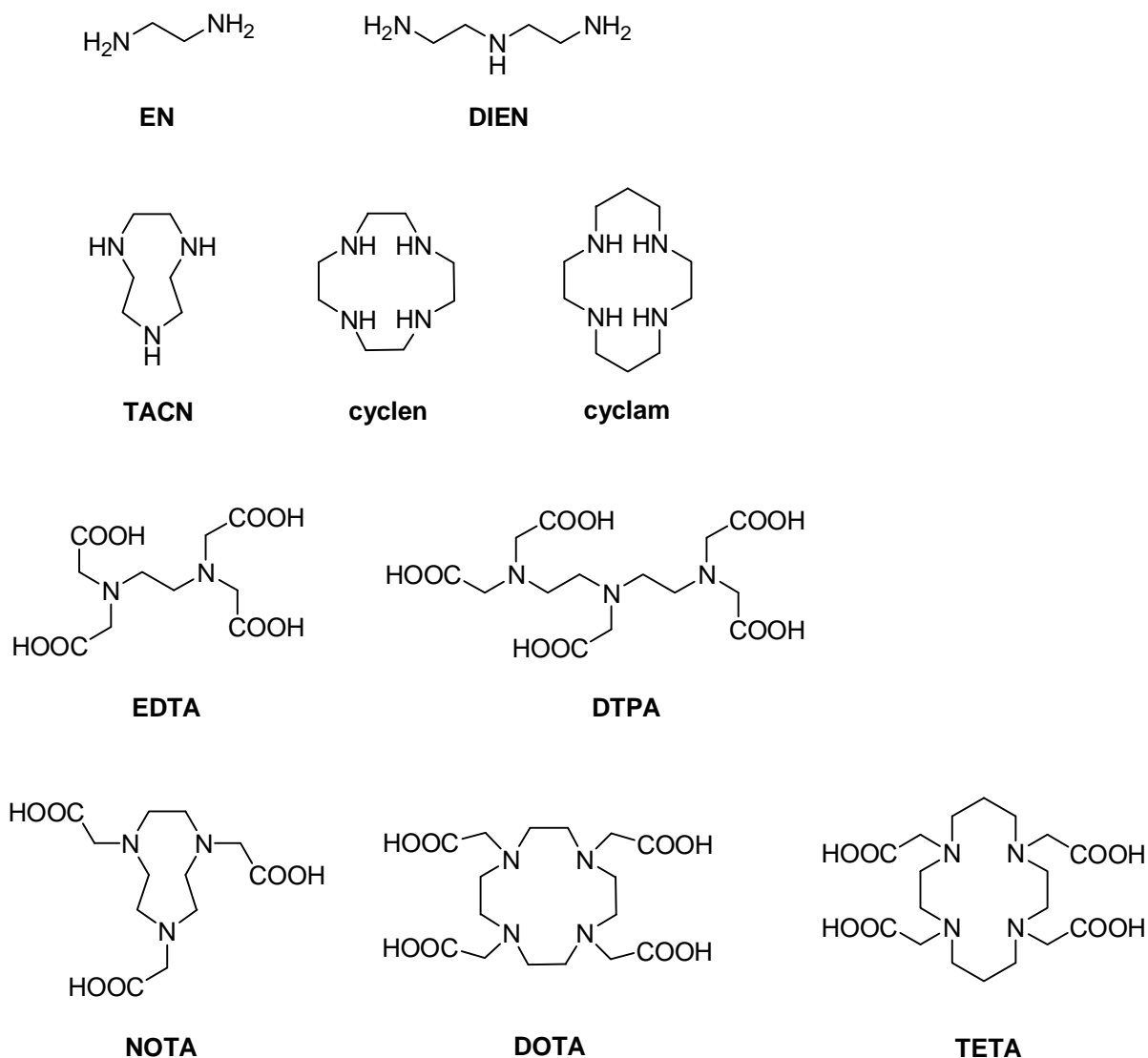


Figure 13. Chemical structures of the studied polyamines.

There are only a few papers about analysis and detection of the above mentioned polyamines, except for EDTA. Most of the methods detect polyamines in form of a metal complex instead of a free ligand [89 – 91]. Since almost none of the polyamines contains a strongly UV-VIS absorbing group, there is a serious need for a simple but efficient derivatization method. Some of the derivatization agents are similar to that used in amino acids derivatization (OPA, FMOC, dansyl, etc.) In this work ten different polyamines (Figure 13) were selected to demonstrate applicability of copper(II) oxide solid-state reactor on improvement of their detection sensitivity by UV-VIS spectrometry. EN and DIEN were chosen as representatives of linear

amines. Both exhibit strongly basic behaviour and chelating ability to majority of transition metals. They are used in organic synthesis for preparation of more complicated compounds including heterocycles, pharmaceuticals and polymers. From the group of cyclic amines TACN, cyclen and cyclam were picked in order to evaluate an influence of a number of nitrogen atoms (TACN has three nitrogen atoms, whereas cyclen and cyclam have four nitrogen atoms) and size of the heterocyclic ring (nine in case of TACN, twelve in case of cyclen and fourteen in case of cyclam). Apart from the simple polyamines, linear and cyclic polycarboxylated amines were studied. Presence of carboxylic groups in their molecules is responsible for different physical as well as coordination properties. Two linear (EDTA and DTPA) and three cyclic (NOTA, DOTA, TETA) polyaminocarboxylates were chosen for the study.

3.2 Experimental

3.2.1 Chemicals

Methanol (gradient grade purity) and copper oxide (p.a. purity grade) were purchased from Merck (Darmstadt, Germany). L-Glycine (Gly), L-alanine (Ala), L-Valine (Val), L-leucine (Leu), L-isoleucine (Ile), L-methionine (Met), L-phenylalanine (Phe), L-tyrosine (Tyr), L-tryptophan (Trp), L-serine (Ser), L-threonine (Thr), L-cysteine (Cys), L-proline (Pro), L-aspartic acid (Asp), L-glutamic acid (Glu), L-asparagine (Asn), L-glutamine (Gln), L-arginine (Arg), L-histidine (His) and L-lysine (Lys) all p.a. purity grade were purchased from Nutritional Biochemicals Corporation (Cleveland, USA). Tris(hydroxymethyl)-aminomethane (TRIS), 1,2-diaminoethane (EN), bis(2-aminoethyl)amine (DIEN) and diethylenetriaminepentaacetic acid (DTPA) all of purity > 98% were supplied by Sigma-Aldrich (Steinheim, Germany). 1,4,7-triazacyclononane (TACN), 1,4,7,10-tetraazacyclododecane (cyclen), both of purity > 98% were supplied by CheMatech (Dijon, France). 1,4,8,11-tetraazacyclotetradecane (cyclam), 1,4,7-triazacyclononane-1,4,7-triacetic acid (NOTA), 1,4,7,10-tetraazacyclododecane-1,4,7,10-tetraacetic acid (DOTA), 1,4,8,11-tetraazacyclotetradecane-1,4,8,11-tetraacetic acid (TETA)

were synthesized at Charles University in Prague, Faculty of Science, Department of Inorganic Chemistry using the modification of synthetic procedures published elsewhere [36]. Acetic acid (98%), hydrochloric acid (p.a. purity grade), disodium ethylenediaminetetraacetate (EDTA, p.a. purity grade), copper sulphate (p.a. purity grade) and sodium hydroxide (p.a. purity grade) were purchased from Lachema (Brno, Czech Republic). Water used in this work was purified with a Milli-Q water purification system (Millipore, USA). Acetate (20 mM, pH 5.5, adjusted with NaOH and 20 mM, pH 4.5, adjusted with NaOH) and TRIS (20 mM, pH 7.0, adjusted with HCl) stock buffer solutions were prepared and stored in refrigerator.

3.2.2 UV-VIS measurements

The UV-VIS experiments were performed on an Agilent DAD 8453 instrument (Waldbronn, Germany) at ambient temperature. All spectra were measured in the range from 200 nm to 800 nm. Spectra of pure EN, DIEN, TACN, cyclen, cyclam, NOTA, DOTA, TETA, EDTA and DTPA (all 1.0×10^{-3} mol/L) were measured in solution of 20 mM acetate buffer (pH 5.5). Spectra of copper complexes with EN, DIEN, TACN, cyclen, cyclam, NOTA, DOTA, TETA, EDTA and DTPA ($c_L = c_M = 1.0 \times 10^{-3}$ mol/L) were measured in solution of 20 mM acetate buffer (pH 5.5). Spectra of the solutions containing L-serine/CuSO₄ in molar ratio 1:1 and 2:1 were measured at pH 5.5 and 7.0 in appropriate buffers.

3.2.3 HPLC instrumentation and conditions

The HPLC experiments were performed on an Ecom liquid chromatograph system (Prague, Czech Republic) comprising of a Beta 10 gradient pump, injection valve with a 10 μ L loop and an LCD 2084 absorbance detector. The system was equipped with an on-line degasser and a mixing chamber. The UV detection was carried out at the wavelength of 230 nm. Analyses were performed on a LiChroCART Purospher STAR RP-18e column (150 \times 4.6 mm I.D., particle size 5 μ m) supplied by Merck (Darmstadt, Germany). A LiChroCART Purospher STAR RP-18e precolumn (4 \times 4.6 mm I.D., particle size 5 μ m) was used to prevent contamination of the analytical column. The chromatograms were recorded and

evaluated through the Clarity 2.6.6. software purchased from DataApex (Prague, Czech Republic). The optimized mobile phase consisted of methanol and buffer solution (20 mM acetate or TRIS; 5:95, v/v). The flow-rate was 0.5 mL/min. All samples were dissolved in the mobile phase. All measurements were carried out at ambient temperature.

Post-column derivatization system

On-line derivatization was carried out using a reactor filled with commercial copper oxide (0.20 g) of average particle size between 1 and 2 μm . Particles shape and size were determined by transmission electron microscopy (TEM). A modified conventional precolumn supplied by Supelco (Bellefonte, USA) was used as the reactor. The precolumn was firstly emptied then refilled with dry derivatization agent and placed after the separation column with a column holder (Supelco, Bellefonte, USA). Stability and capacity of the reactor was tested by flushing with EDTA solution (1.0×10^{-3} mol/L, 720 mL, i.e. flushing for 24 hours using a flow-rate of 0.5 mL/min).

Detection sensitivity study

Detector responses of all 20 amino acids (1.0×10^{-3} mol/L) were measured firstly without any derivatization and then after passing through the CuO solid-state reactor. The mobile phase used consisted of methanol and buffer solution (20 mM acetate or TRIS; 5:95, v/v). All measurements were carried out in triplicates and the mean peak areas were taken into account. Four amino acids (L-valine, L-serine, L-glutamic acid and L-histidine) were chosen for detailed study. Calibration curves within the concentration interval of 5.0×10^{-4} to 1.0×10^{-2} mol/L for underivatized L-valine, L-serine and L-glutamic acid were measured under the optimized separation conditions described above. Due to the higher response of underivatized L-histidine, the calibration curve of this amino acid was studied within the concentration interval of 1.0×10^{-5} to 5.0×10^{-3} mol/L. Then calibration curves within the concentration interval of 5.0×10^{-5} to 2.0×10^{-3} mol/L of L-valine, L-serine, L-glutamic acid and L-histidine were measured using the post-column

derivatization. Calibration curves were measured at two different pH values – pH 5.5 and 7.0. The measurements at all concentrations and pH values were carried out in triplicates and the mean peak areas were plotted against the analyte concentration and subjected to linear regression using the least squares method to obtain individual parameters of the calibration lines. Statistic significance of intercepts (a) was tested using t -test at significance level of $\alpha = 0.01$ (i.e., $t = a/SDa$; SDa is standard deviation of a). Statistic evaluation of experimental data was performed by Microsoft Excel 2002.

Flow rate effect

L-Serine ($c = 2.0 \times 10^{-3}$ mol/L) and mobile phase consisted of methanol and 20 mM acetate buffer (pH 5.5, adjusted with NaOH) (5:95, v/v) were employed. The tested flow-rates ranged from 0.2 to 1.3 mL/min. The same experiments were performed with all the tested polyamines except cyclen ($c = 1.0 \times 10^{-3}$ mol/L). Due to lower absorption of cyclen system, the concentration used for the flow-rate effect study was 1.0×10^{-2} mol/L.

Derivatization efficiency study

The experiment was performed on HPLC system using a special setup. The separation column and the post column reactor were removed and the HPLC pump was directly connected to the UV-VIS detector through an empty fused silica capillary with 320 μ m I.D. Solutions of L-serine (1 mM) with various amount of CuSO_4 (molar ratio Cu(II)/L-serine ranging from 0.05 to 0.5) were injected. The measurements were taken at pH 5.5 and 7.0. Flow-rate of 0.5 mL/min was applied.

Applicability study

Detector responses of EN, DIEN, TACN, cyclen, cyclam, NOTA, DOTA, TETA, EDTA and DTPA (all 1.0×10^{-3} mol/L) were measured firstly without any derivatization and then after passing through the copper(II) oxide solid-state reactor. Mobile phases of the three different pH values (4.5, 5.5 and 7.0) were employed. The mobile phases used consisted of methanol and buffer solution (20 mM acetate for pH

4.5 and 5.5 or 20 mM TRIS for pH 7.0; 5:95, v/v). Detection was carried out at wavelength of 230 nm. Then detector responses of all the 10 polyaminocarboxylates were measured after solid-state derivatization at optimal wavelengths (ranging from 230 to 310 nm, see Table 11, page 62). This experiment was performed in a mobile phase consisting of methanol and 20 mM acetate buffer (pH 5.5, adjusted with NaOH) (5:95, v/v). All measurements were carried out in triplicates and the mean peak areas were taken into account.

3.3 Results and discussion

3.3.1 Amino acids derivatization

The presented post-column derivatization for UV-VIS detection of amino acids and other polyamines was realized with a reactor filled with copper(II) oxide powder. It is well known that many amino acids are almost non-absorbing in UV region and can be detected only at very short wavelengths (190 – 210 nm) with a rather low response. However, their Cu(II) complexes enable detection in the UV region (220 nm to 240 nm) due to intensive charge-transfer bands. As amino acids are good complexation agents showing high affinity for Cu(II) ions, they have the ability to fish out copper atoms from insoluble compounds. Therefore, the interaction of analytes with CuO leads to the formation of corresponding complexes and consequent increase of UV-VIS detection sensitivity, as it is illustrated on the calibration curves of L-serine (Figure 14).

Wavelength of 230 nm was chosen as the optimal wavelength for detection, due to a reasonable absorbance of the Cu(II) complexes (for UV-VIS spectra see Figure 15). Moreover, the chosen wavelength is long enough to avoid the problems generally associated with the detection around 200 nm like high system peaks or absorption of the mobile phase.

The derivatization efficiency was tested for all 20 proteinogenic amino acids. Significant increase of the detector response of all analytes was observed upon derivatization (Figure 16). For amino acids having no strongly absorbing group, derivatization results in two to four orders of magnitude sensitivity increase. Even for strongly absorbing analytes as L-histidine and L-tryptophan, derivatization led to a

considerable sensitivity increase of one order of magnitude. To get deeper insight into the topic, derivatization was studied in detail for four amino acids, namely: L-valine as an amino acid with a hydrophobic side chain, L-serine as a representative of polar amino acids, L-histidine as a representative of basic amino acids and L-glutamic acid as one of acidic amino acids. The results are summarized in Table 7.

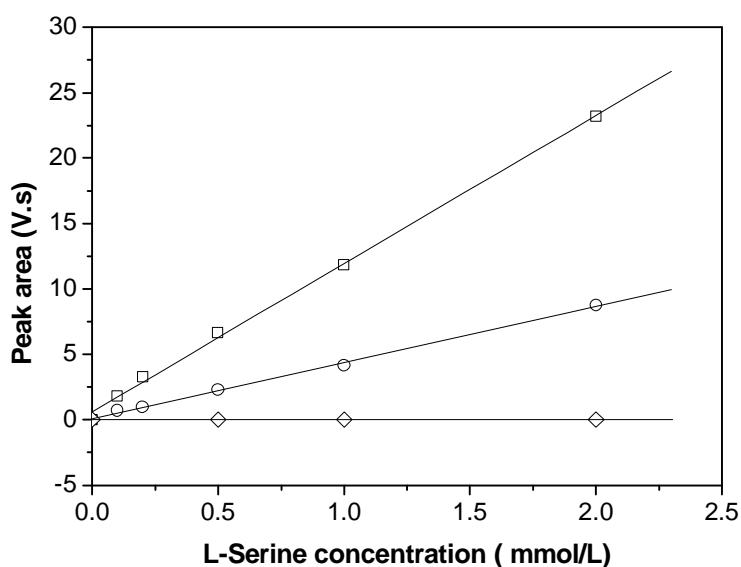


Figure 14. Calibration curves of L-serine after CuO post-column derivatization measured at pH 5.5 (□) and 7.0 (○). Only one calibration curve without derivatization (◇) is displayed because comparable curves were obtained for both pH values. Conditions: Purospher STAR RP-18e column, mobile phase – methanol and buffer solution (acetate or TRIS; 5:95, v/v), detection at $\lambda = 230$ nm.

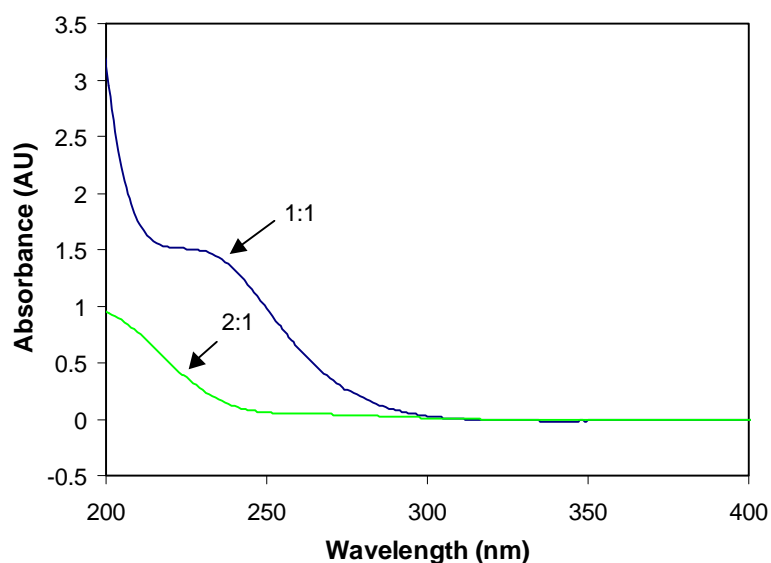


Figure 15. UV-VIS spectra of the solutions containing Cu(II) complexes with L-serine. $c_M = c_L = 0.5$ mmol/L, acetate buffer pH 5.5 (blue); $c_M = 0.5$ mmol/L, $c_L = 0.25$ mmol/L TRIS buffer pH 7.0 (green). Spectra were measured at ambient temperature.

Table 7. The sensitivities of detection expressed as calibration line slopes. Conditions: Purospher STAR RP-18e column, mobile phase – methanol and buffer solution (acetate or TRIS; 5:95, v/v), flow-rate 0.5 mL/min.

Amino acid	Without derivatization Slope (V.s.L/mol)		After derivatization Slope (V.s.L/mol)		Increase of sensitivity	
	pH = 5.5	pH = 7.0	pH = 5.5	pH = 7.0	pH = 5.5	pH = 7.0
L-Valine	1.32×10^4	1.08×10^4	1.38×10^7	6.69×10^6	1045	620
L-Serine	1.47×10^4	1.40×10^4	1.11×10^7	4.25×10^6	755	304
L-Histidine	1.97×10^6	1.80×10^6	1.83×10^7	9.03×10^6	9.3	5.1
L-Glutamic acid	1.77×10^4	2.01×10^4	5.40×10^6	1.28×10^6	305	64

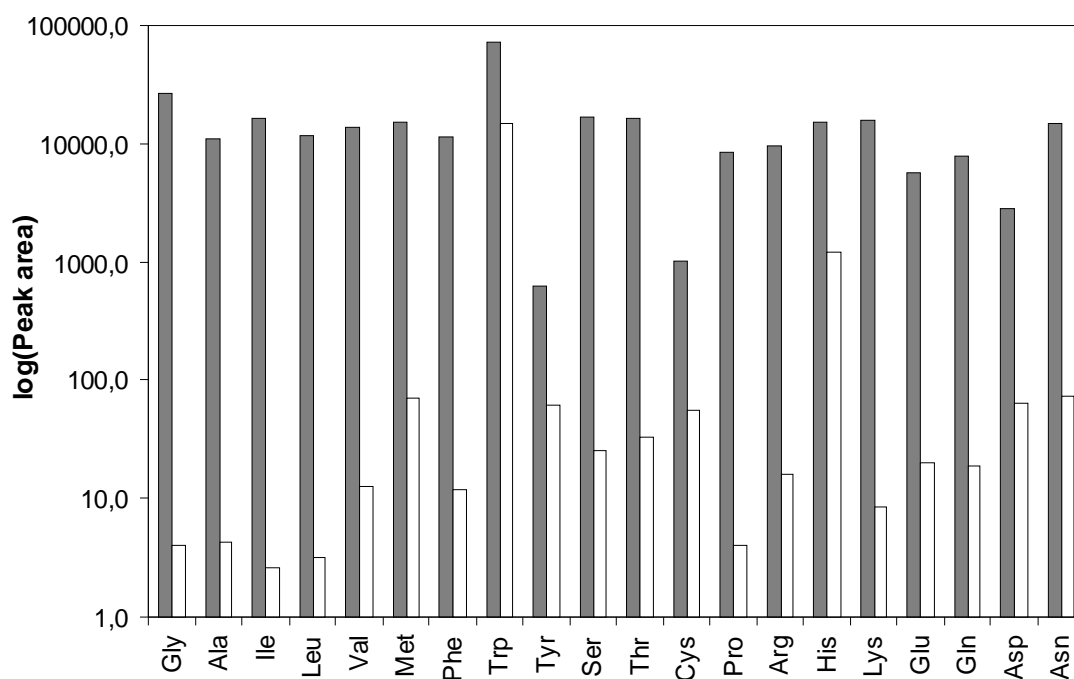


Figure 16. Comparison of the detector response for 20 proteinogenic amino acids obtained after CuO post-column derivatization (grey) and without derivatization (white). Conditions: Purospher STAR RP-18e column, mobile phase consisted of methanol and acetate buffer solution, 5:95 v/v, the flow-rate was 0.5 mL/min; $c = 1.0 \times 10^{-3}$ mol/L, detection at $\lambda = 230$ nm. Detector response is presented in logarithmic scale.

Due to a higher degree of the dissociation of the amino group, amino acids exhibit stronger coordination ability at higher pH values. Despite that, the detection efficiency observed at pH 7.0 is approximately 50% lower than that observed at pH 5.5. This is due to differing distribution of the complex species [92] (for distribution diagrams see Figure 17) at different pH. At pH 5.5, complexes with 1:1 ligand to metal ratio are predominantly formed even under excess of the ligand. On the contrary, at pH 7.0, amino acids form predominantly 2:1 ligand to metal complexes. Thus, at higher pH, only half the amount of copper(II) ions is complexed with the same amount of amino acid, which leads to the lower sensitivity observed.

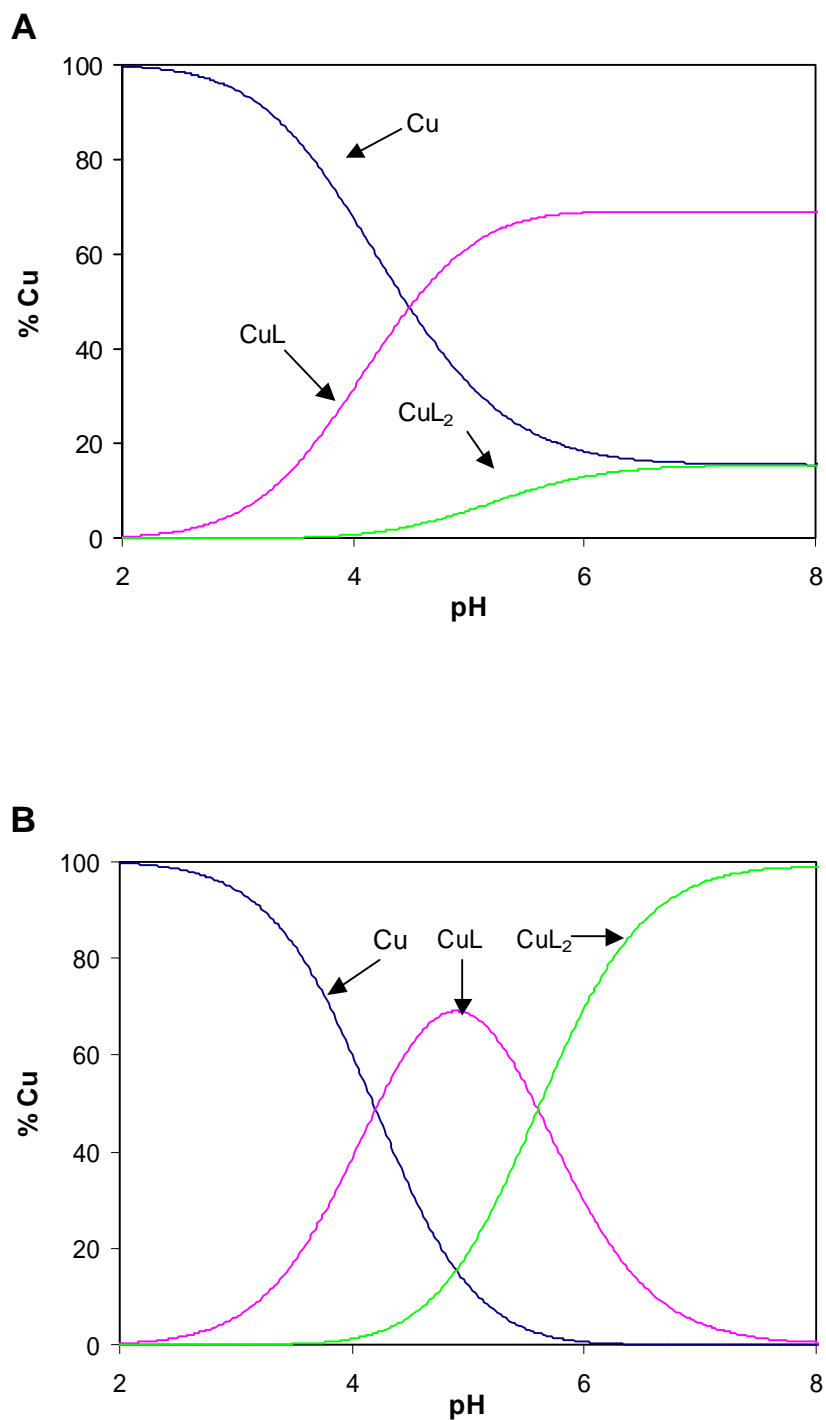


Figure 17. Distribution diagrams of the L-serine/Cu(II) complex based on published thermodynamic constants [92] and plotted using Opium program package [93]. $c_M = c_L = 0.004 \text{ mol/L}$ (A); $c_M = 2.0 \times 10^{-3} \text{ mol/L}$, $c_L = 4.0 \times 10^{-3} \text{ mol/L}$ (B).

The increase of the detection sensitivity is proportional to the amount of Cu(II) complex formed while the analyte passes through the reactor zone. The reaction of the analyte with an excess of solid CuO resembles zero-order kinetics and, so, the yield of the derivatization is determined mainly by the flow-rate. In case of slow complex formation, the signal should be proportional to the contact time, whereas in case of fast complex formation, the analyte is “saturated” with copper and the signal intensity should not change with the contact time. The influence of the flow-rate on the derivatization was studied in the range of 0.2 – 1.3 mL/min. Normalized peak area (area multiplied by flow-rate to eliminate impact of the flow-rate change on the peak area) plotted against inverse value of the flow-rate (proportional to the contact time) is depicted in Figure 18. The saturation shape of the curve is in a good agreement with the expectation. The results show that the complex formation is fast and more than 85% of the signal maximal value is reached under all applied flow-rates. It indicates that the developed post-column derivatization is perfectly suitable for the flow-rates typical for HPLC systems (0.5 – 1.0 mL/min).

To further investigate the complexation efficiency, a special setup of the HPLC system was utilized as follows: An empty fused silica capillary was used instead of the HPLC column and the solid-state reactor. Constant amount of L-serine together with variable amounts of Cu(II) were injected and the resulting peak areas were compared with the peak areas obtained for similar L-serine samples upon derivatization at the same flow-rate. These experiments on derivatization efficiency have shown that the derivatization leads to the Cu(II) content corresponding to 80% and 40% of the injected amount of amino acid at pH 5.5 and pH 7.0, respectively. These results provide further confirmation of the high degree of complexation and the preference for the species with different ligand to metal ratio in both experiments. Similar results on derivatisation efficiency were obtained also for other studied amino acids.

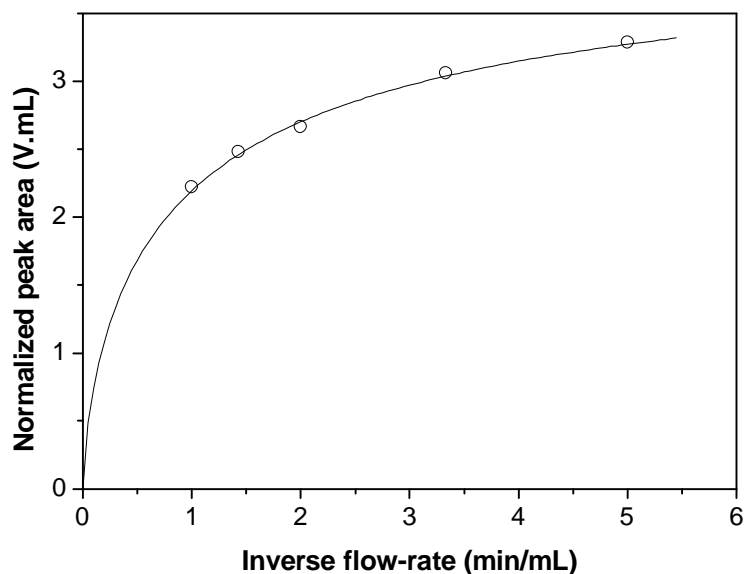


Figure 18. Dependence of the normalized peak area on the inverse value of the flow rate. The curve is for guiding eyes only. Conditions: L-serine ($c = 2.0 \times 10^{-3}$ mol/L), Purospher STAR RP-18e column, mobile phase consisted of methanol and acetate buffer solution, 5:95 v/v, detection at $\lambda = 230$ nm.

The use of the post-column derivatization has no negative impact on the quality of the analysis. The correlation coefficients perfectly limit to 1.00 for all the calibration curves. None of the intercepts of the calibration lines was found to be significantly different from zero, with a significance level of $\alpha = 0.01$ applying the *t*-test for intercepts [41]. For complete calibration parameters see Tables 8 and 9. The repeatability of the optimized method with post-column derivatization was compared to that of the analyses without derivatization step. There was no significant difference between RSDs values of the peak area and the peak height. The values of both RSDs were around 3.8% for underivatized samples. In case of derivatized samples, RSDs descended even lower (2.8%) providing an outstanding repeatability. The day-to-day repeatability of the post-column derivatization method was almost as good as that of the run-to-run one (RSDs around 5%).

Table 8. Parameters of the calibration curves obtained by measurements under the optimized conditions without derivatization. Conditions: Purospher STAR RP-18e column, mobile phase consisted of methanol and acetate or TRIS buffer solution, 5:95 v/v, the flow-rate was 0.5 mL/min.

Amino acid	pH = 5.5			pH = 7.0		
	Slope (V.s.L/mol)	Intercept $\times 10^{-3}$ (V.s)	<i>r</i>	Slope (V.s.L/mol)	Intercept $\times 10^{-3}$ (V.s)	<i>r</i>
Val	1.32×10^4	- 2.3	0.999	1.08×10^4	4.0	0.998
Ser	1.47×10^4	14.3	0.996	1.40×10^4	- 0.9	0.997
His	1.97×10^6	- 5.9	0.999	1.80×10^6	- 7.7	0.999
Glu	1.77×10^4	12.8	0.997	2.11×10^4	9.5	0.996

Table 9. Parameters of the calibration curves obtained by measurements under optimal conditions after the CuO post-column derivatization. Conditions: Purospher STAR RP-18e column, mobile phase consisted of methanol and buffer solution (acetate or TRIS; 5:95, v/v), the flow-rate was 0.5 ml/min.

Amino acid	pH = 5.5			pH = 7.0		
	Slope (V.s.L/mol)	Intercept $\times 10^{-3}$ (V.s)	<i>r</i>	Slope (V.s.L/mol)	Intercept $\times 10^{-3}$ (V.s)	<i>r</i>
Val	1.38×10^7	- 13.9	0.999	6.69×10^6	94.2	0.997
Ser	1.11×10^7	711.2	0.999	4.25×10^6	137.3	0.998
His	1.83×10^7	- 817.6	0.996	9.03×10^6	- 147.3	0.998
Glu	5.41×10^6	1012.0	0.995	1.28×10^6	172.6	0.997

Stability of the CuO solid-state reactor was further tested by flushing the reactor with EDTA solution. After passing the molar amount of EDTA being equivalent to more than 70,000 injections, the detector response decreased by approximately 15%. Such result confirms a high reproducibility of derivatization over a long period of time and over a huge number of analyses.

The LOD and LOQ values of the presented detection method are depicted in Table 10. Generally, sensitivity of the detection is in pmol range for MS techniques [94] and in pmol and fmol range for UV-VIS and LIF detection after homogeneous derivatization when using ninhydrin, OPA, PITC, FMOC and dansyl chloride [95]. The sensitivity of quantification reached with UV-VIS detection after the solid-phase derivatization in this study is in nmol and pmol range. Moreover, the presented method of derivatization profits from simplicity of realization, low costs and minimization of the negative effects usually introduced by derivatization. Furthermore, the solid-phase derivatization method brings significant improvement of UV-VIS detection without any special requirements on equipment and operation time.

Table 10. Performance parameters of the calibration curves obtained by measurements under optimized conditions after the CuO derivatization. Conditions: Purospher STAR RP-18e column, mobile phase consisted of methanol and acetate or TRIS buffer solution, 5:95 v/v, the flow-rate was 0.5 mL/min.

Amino acid	pH = 5.5			pH = 7.0		
	LOD (mol/L)	LOQ (mol/L)	Linearity factor	LOD (mol/L)	LOQ (mol/L)	Linearity factor
Val	1.28×10^{-6}	4.28×10^{-6}	1.02	2.69×10^{-6}	8.95×10^{-6}	0.99
Ser	2.60×10^{-6}	8.67×10^{-6}	0.96	3.62×10^{-6}	1.21×10^{-5}	0.94
His	1.78×10^{-6}	6.01×10^{-6}	1.07	3.53×10^{-6}	1.18×10^{-5}	1.06
Glu	4.56×10^{-6}	1.62×10^{-5}	0.91	1.25×10^{-5}	4.17×10^{-6}	1.02

3.3.2 Applicability study

As described above, the newly developed post-column solid-state reactor based on copper(II) oxide powder was successfully tested for 20 proteinogenic amino acids. Nevertheless, there is a wide scope of other compounds capable of complexing copper that are potential analytes for this reactor. In the second part of this study, the reactor applicability to other analytes was evaluated. The row of linear and cyclic polyamines as well as linear and cyclic polyaminocarboxylates was chosen for this purpose (see Figure 13, page 46).

The UV-VIS behaviour of polyamines is very similar to that of amino acids. As the polyamines lack in their molecules any strong chromophore, their absorption maximum lies under 200 nm. That brings exactly the same problems into the UV-VIS detection as in case of amino acids. Similarly to amino acids, they easily form copper(II) complexes that can be used for more sensitive UV-VIS detection. Such complexes have maximum of absorbance ranging from 230 to 310 nm (Figures 19, 20 and 21). The optimal detection wavelengths of each polyamine-copper(II) complex are summarized in Table 11. Unlike amino acid, the wavelength of maximum absorbance differs significantly for each polyamine. That is caused by variations in the structure of studied polyamines and consequently different arrangement of a coordination sphere of the complex. In order to obtain results, which would readily be comparable with each other and also with data obtained for amino acids previously, the polyamines were tested at wavelength 230 nm. The fact that the chosen detection wavelength did not correspond with the optimum (especially for cyclen, DOTA and TETA) had no influence on the trends observed during this study. The highest possible detector response was also measured for all the studied analytes and will be discussed later.

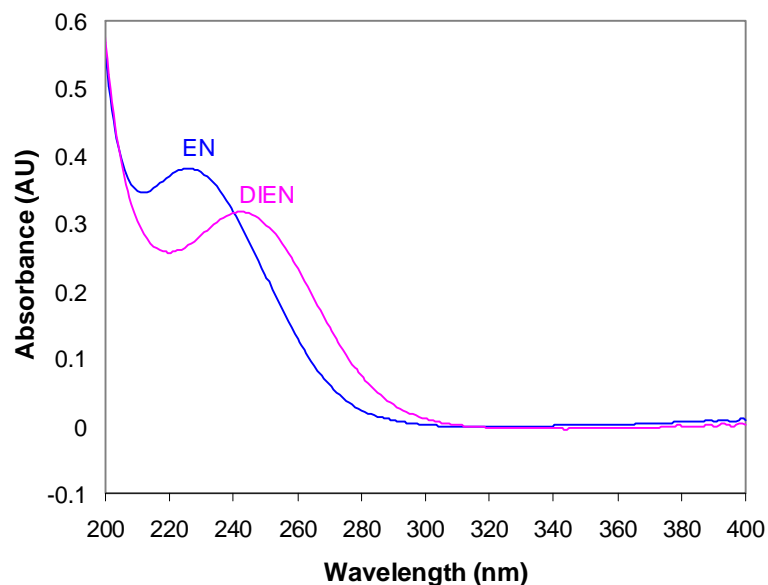


Figure 19. Spectra of copper(II) complexes with linear polyamines (EN, DIEN) as ligands. $c_L = c_M = 1.0 \times 10^{-3}$ mol/L. Spectra were measured in solution of 20 mM acetate buffer (pH 5.5) at ambient temperature.

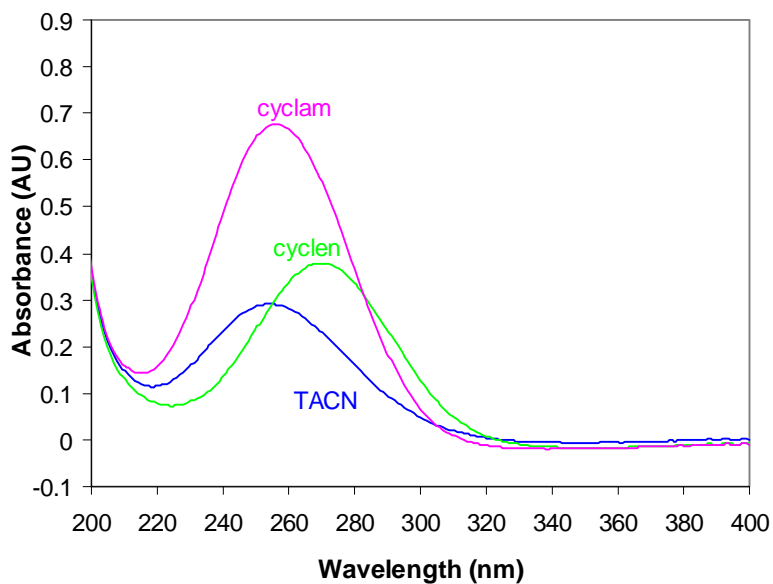


Figure 20. Spectra of copper(II) complexes with cyclic polyamines (cyclen, cyclam, TACN) as ligands. $c_L = c_M = 1.0 \times 10^{-3}$ mol/L. Spectra were measured in solution of 20 mM acetate buffer (pH 5.5) at ambient temperature.

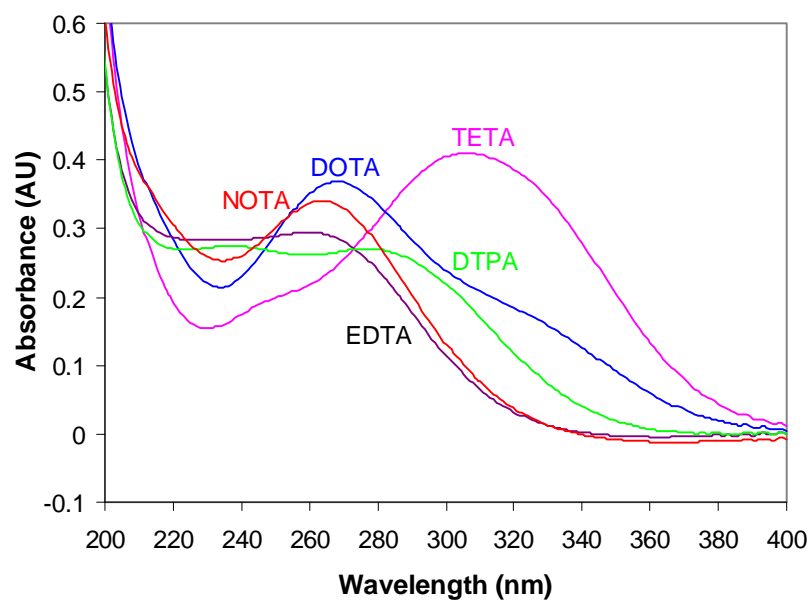


Figure 21. Spectra of copper(II) complexes with polyaminocarboxylates (EDTA, DTPA, NOTA, DOTA, TETA) as ligands. $c_L = c_M = 1.0 \times 10^{-3}$ mol/L. Spectra were measured in solution of 20 mM acetate buffer (pH 5.5) at ambient temperature.

Table 11. The optimal detection wavelengths of polyamines.

	Wavelength (nm)		Wavelength (nm)
EN	230	EDTA	260
DIEN	245	DTPA	240
TACN	250	NOTA	260
cyclen	270	DOTA	270
cyclam	260	TETA	310

Since polyamines and polyaminocarboxylates contain from two to eight groups that could either be protonized or deprotonized, the pH value of the mobile phase could influence their degree of dissociation and consequently derivatization

itself. Therefore mobile phases containing buffers of three different pH values (4.5, 5.5 and 7.0) were employed to find the optimal pH for the derivatization. The results show (Figure 22) that there is no one optimal pH value for all analytes. In case of cyclen, cyclam, TETA and partly DOTA, the pH value of a mobile phase does not seem to be principal. For the rest of the tested samples, higher pH (5.5 or 7.0) is more convenient as it provides an increase of detector response. The pH value 7.0 was found to be optimal for solid-state derivatization of simple linear polyamines (EN, DIEN) and EDTA, whereas pH 5.5 seems to be optimal for TACN and DTPA.

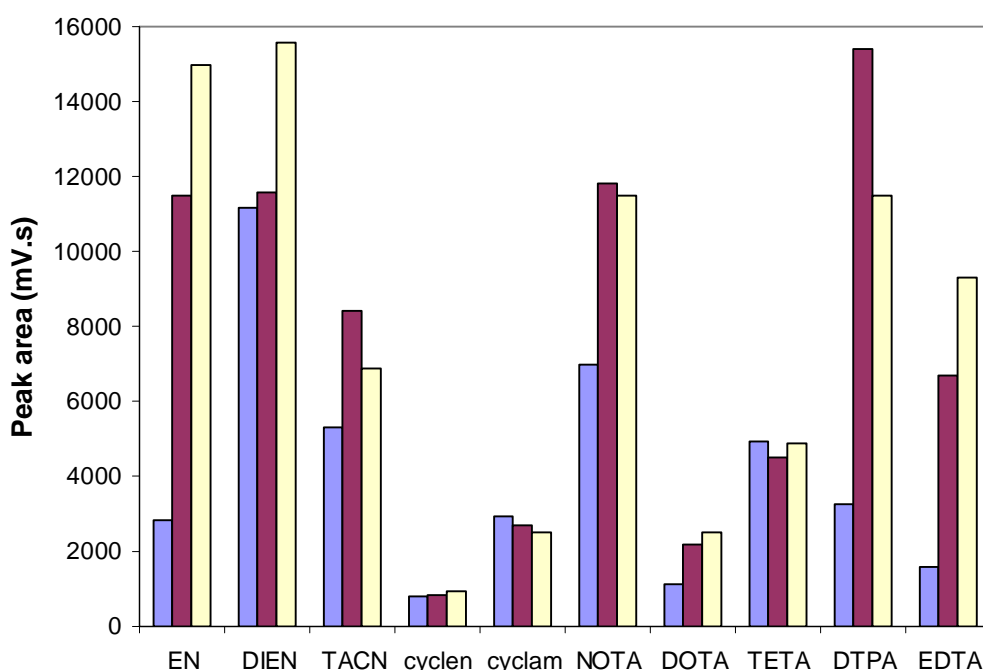


Figure 22. Comparison of the detector response of the ten polyamines obtained after CuO post-column derivatization at pH 4.5 (blue), 5.5 (red) and 7.0 (yellow). Conditions: Purospher STAR RP-18e column, mobile phase consisted of methanol and acetate or TRIS buffer solution, 5:95 v/v, the flow-rate was 0.5 mL/min; $c = 1.0 \times 10^{-3}$ mol/L, detection at $\lambda = 230$ nm.

To generalize, prediction of optimal pH value for derivatization is complicated. There is no straight relation between the structure of polyamines and

the optimal pH value of a mobile phase. Nevertheless, pH optimization is worth of trying as it could lead to a considerable increase of a detector response. The experimental results show that the derivatization is in majority of cases most efficient between pH 5.5 and 7.0. The difference in detector response, when applied mobile phases of these two pH values, is no more than 30% for any of the tested compounds. A switchover from mobile phase with pH 5.5 to mobile phase of pH 4.5 brings difference in detector response even up to 80% for some of the tested analytes.

Based on the assumption that polyamines exhibit similar behaviour to amino acids, the yield of derivatization should be determined by the applied flow-rate. To confirm this hypothesis, the influence of the flow-rate on the detection sensitivity was tested in range from 0.2 to 1.3 mL/min. The results of the studied linear, cyclic and carboxylated polyamines are depicted in Figures 23, 24 and 25, respectively.

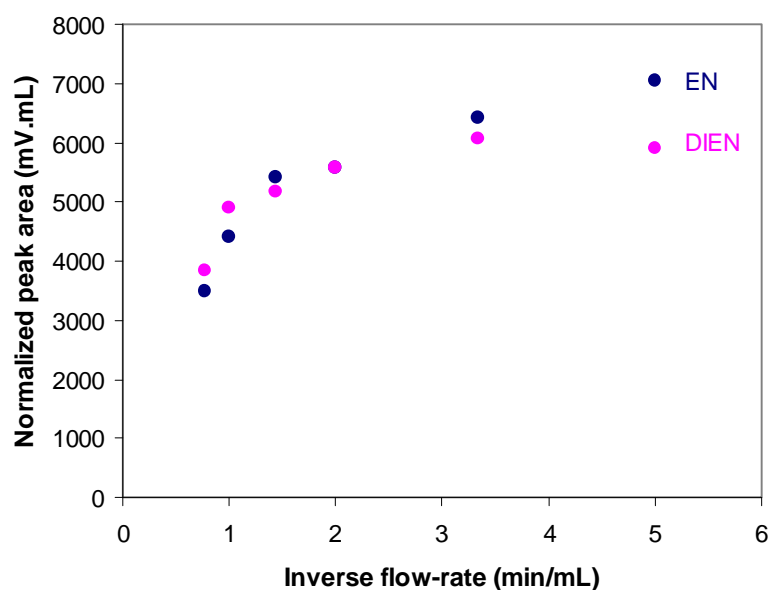


Figure 23. Dependence of the normalized peak area of the linear polyamines on the inverse value of the flow rate. Conditions: Purospher STAR RP-18e column, mobile phase consisted of methanol and acetate buffer solution (pH = 5.5), 5:95 v/v, the flow-rate was 0.5 mL/min; $c = 1.0 \times 10^{-3}$ mol/L, detection at $\lambda = 230$ nm.

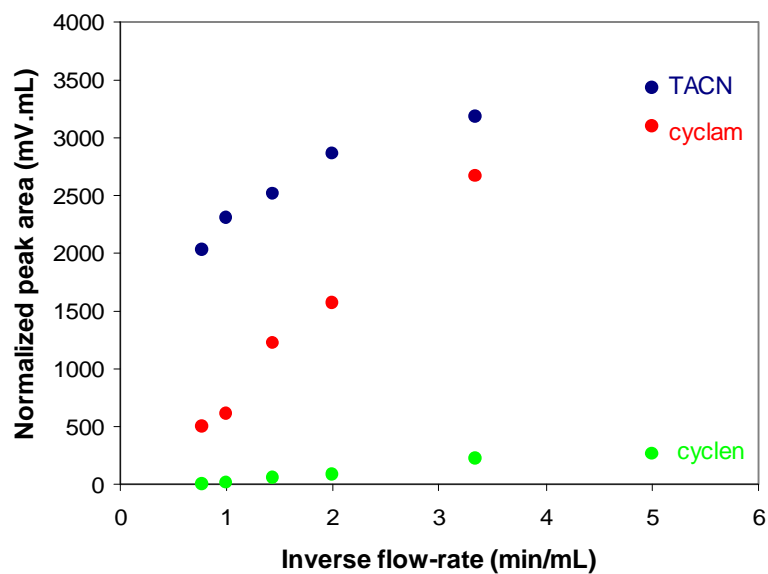


Figure 24. Dependence of the normalized peak area of the cyclic polyamines on the inverse value of the flow rate. Conditions: Purospher STAR RP-18e column, mobile phase consisted of methanol and acetate buffer solution (pH = 5.5), 5:95 v/v, the flow-rate was 0.5 mL/min; $c = 1.0 \times 10^{-3}$ mol/L, detection at $\lambda = 230$ nm.

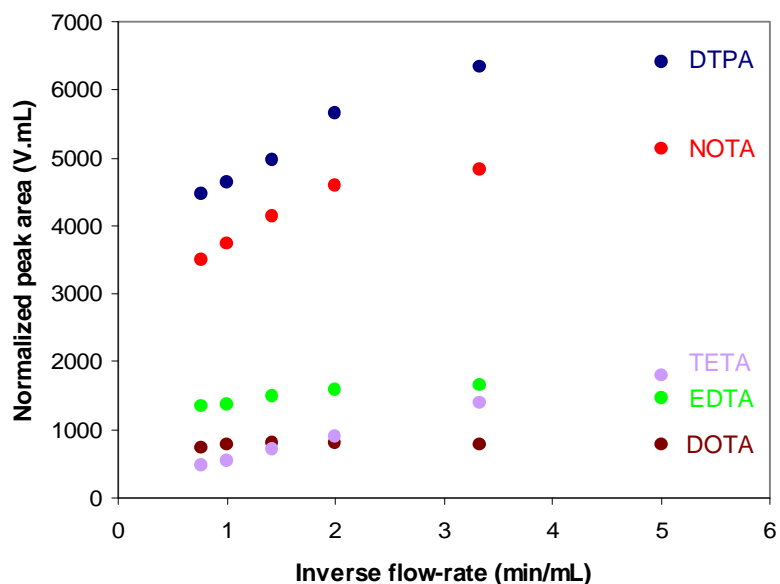


Figure 25. Dependence of the normalized peak area of the carboxylated polyamines on the inverse value of the flow rate. Conditions: Purospher STAR RP-18e column, mobile phase consisted of methanol and acetate buffer solution (pH = 5.5), 5:95 v/v, the flow-rate was 0.5 mL/min; $c = 1.0 \times 10^{-3}$ mol/L, detection at $\lambda = 230$ nm.

There are significant differences among the tested polyamines. The behaviour of both simple linear polyamines (EN and DIEN), simple cyclic polyamine TACN and two of the polyaminocarboxylates (DTPA, NOTA) precisely resembles the curve obtained for amino acids (see Figure 18, page 57). The complex formation of these compounds is fast and the analyte is “saturated” with copper(II) at flow-rates under 0.5 mL/min. It means that the signal intensity does not change when applied even lower flow-rates. Cyclen and cyclam from the group of cyclic polyamines and polyaminocarboxylate TETA exhibit different complexation behaviour. The detector response of these compounds does not reach any saturation plateau. This behaviour signifies that formation of copper(II) complexes is slow and detector response is proportional to the contact time of analyte with the derivatization agent. The rest of the tested polyamines i.e. polyaminocarboxylates EDTA and DOTA, show an opposite behaviour to the previous group of compounds. As emerge from the flat shape of the curve in Figure 25, these compounds reach the complete saturation even at the highest tested flow-rate. Therefore, their signal cannot be arised by any prolongation of the contact time of analyte with the derivatization agent.

As already mentioned above, selection of a proper detection wavelength is of the significant importance when analyzing polyamines. This fact is clearly illustrated in Figure 26. The detector response of each studied polyamine was measured at its optimal wavelength using a mobile phase of pH 5.5 (the optimal detection wavelengths are summarized in Table 11, page 62). The most noticeable difference between the optimal and the “standard” detection wavelength (i.e. 230 nm) was observed for cyclen, DOTA and TETA. In these three cases, the signal at the wavelength of 230 nm was only 20% of the maximal possible value. On the other hand, a negligible difference occurred in case of EN, DIEN and DTPA due to vicinity of their optimal wavelength to the “standard” wavelength of 230 nm.

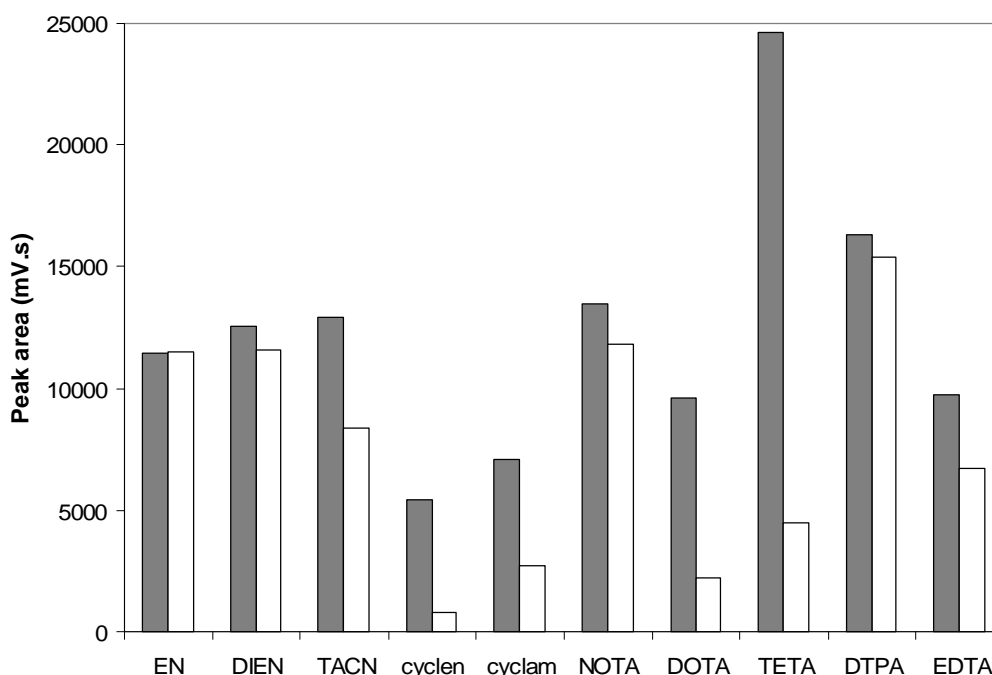


Figure 26. Comparison of the detector responses measured at optimal wavelength (grey) and standard wavelength of 230 nm (white). Conditions: Purospher STAR RP-18e column, mobile phase consisted of methanol and acetate buffer solution (pH = 5.5), 5:95 v/v, the flow-rate was 0.5 mL/min; $c = 1.0 \times 10^{-3}$ mol/L.

A significant increase of the detector response was observed for all of the studied polyamines upon the solid-state derivatization (Figure 27). The detection sensitivity of the polyaminocarboxylates, regardless linear or cyclic, was increased approximately by one order of magnitude. For the rest of polyamines, the solid-state derivatization resulted in sensitivity increase of two orders of magnitude. These results provide a clear evidence of the reactor usability for wide variety of analytes capable of complexing copper.

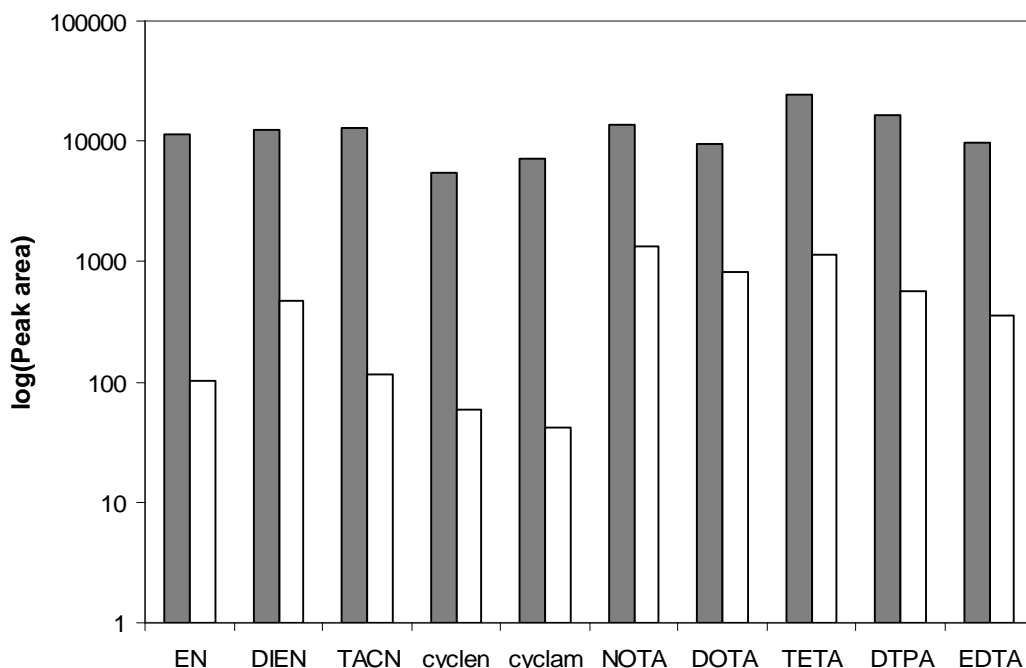


Figure 27. Comparison of the detector response for the tested polyamines obtained after CuO post-column derivatization (grey) and without derivatization (white). Conditions: Purospher STAR RP-18e column, mobile phase consisted of methanol and acetate buffer solution, 5:95 v/v, the flow-rate was 0.5 mL/min; $c = 1.0 \times 10^{-3}$ mol/L. Detector response is presented in logarithmic scale.

3.4 Conclusion

In this work, a novel HPLC post-column derivatization system based on the reaction of analytes with copper(II) oxide in the solid-state reactor has been developed. The derivatization significantly improves applicability of UV-VIS spectrometry for the detection of UV-VIS non-responding analytes capable of complexing copper. The reactor was tested for amino acids and polyamines, but it might readily be used also for other compounds such as peptides. After derivatization, the detection sensitivity of amino acids has increased by two to four orders of magnitude when compared to analyses without the derivatization step. The

increase in detection sensitivity for the polyamines tested was lower than for amino acids, but still considerable with improvement of one to two orders of magnitude.

The solid-phase reactor is highly stable during a long period of time and large number of injections. Moreover, almost no adverse effects on the quality of analyses were observed since only negligible peak broadening occurred. To summarize, the presented derivatization method represents a simple, efficient and economical way of detecting a wide variety of “invisible” compounds by the UV-VIS spectrometry.

Concluding summary

This dissertation thesis has clearly demonstrated HPLC and CZE as powerful separation tools for the analysis and quantification of polyamines and polycarboxylates, however, these techniques need to be provided with a sensitive detection method. The developed online post-column solid-phase derivatization combined with a common UV-VIS detector does accomplish as much as necessary the sensitivity requirement.

REFERENCES

- [1] J. McMurry, *Organic chemistry (Sixth edition)*, Brooks/Cole, Belmont, 2004.
- [2] R. K. Murray, D. K. Granner, P. A. Mayes, V. W. Rodwell, *Harper's Biochemistry*, Appleton & Lange, East Norwalk, 1993.
- [3] T. M. Devlin, *Biochemistry with Clinical Correlations*, Wiley-Liss, New York 1992.
- [4] C. B. Anfinsen, J. T. Edsall, F. M. Richards, *Advances in Protein Chemistry*. New York: Academic Press., New York, 1972.
- [5] A. J. P. Martin, R. L. M. Synge, *Biochem. J.* **1941**, 35, 1358.
- [6] D. H. Spackman, W. H. Stein, S. Moore, *Anal. Chem.* **1958**, 30, 1190.
- [7] F. A. Cotton, G. Wilkinson, C. A. Murillo, M. Bochman, *Advanced inorganic chemistry*, Wiley, Chichester, 1999.
- [8] J. A. Makašev, V. M. Zamjatkinová, *Sloučeniny v hranatých závorkách*, (J. Sikač, Czech translation), Polytechnická knihnice, Praha, 1981.
- [9] A. E. Merbach, E. Tóth, *The Chemistry of Contrast Agents in Medical Magnetic Resonance Imaging*, Wiley, Chichester, 2001.
- [10] P. Caravan, J. J. Ellison, T. J. McMurry, R. B. Lauffer, *Chem. Rev.* **1999**, 99, 2293.
- [11] M. J. Welch, C. S. Redvanly, *Handbook of Radiopharmaceuticals. Radiochemistry and Applications*, Wiley, Chichester, 2003.
- [12] B. J. Pichler, H. F. Wehrl, M. S. Judenhofer, *J. Nucl. Med.* **2008**, 49, 5S.
- [13] M. S. Rosenthal, J. Cullom, W. Hawkins, S. C. Moore, B. M. W. Tsui, M. Jester, *J. Nucl. Med.* **1995**, 39, 1489.
- [14] C. J. Anderson, M. J. Welch, *Chem. Rev.* **1999**, 99, 2219.
- [15] P. Caravan, *Chem. Soc. Rev.* **2006**, 35, 512.
- [16] S. G. Crich, A. Barge, E. Battistini, C. Cabella, S. Coluccia, D. Longo, V. Mainero, G. Tarone, S. Aime, *J. Biol. Inorg. Chem.* **2005**, 10, 78.
- [17] S. Aime, C. Cabella, S. Colombatto, S. G. Crich, E. Gianolio, F. Maggioni *J. Magn. Reson. Imaging* **2002**, 16, 394.

- [18] N. R. Sibson, A. M. Blamire, M. Bernades-Silva, S. Laurent, S. Boutry, R. N. Muller, P. Styles, D. C. Anthony *Magn. Reson. Med.* **2004**, *51*, 248.
- [19] V. Kubíček, J. Rudovský, J. Kotek, P. Hermann, L. V. Elst, R. N. Muller, Z. I. Kolar, H. T. Wolterbeek, J. A. Peters, I. Lukeš, *J. Am. Chem. Soc.* **2005**, *127*, 16477.
- [20] C. Y. Chang, D. Silverman, *Expert Rev. Mol. Diagn.* **2004**, *4*, 63.
- [21] M. S. Albert, *Alzheimer Dis. Assoc. Disord.* **2003**, *17*, S63.
- [22] W. E. Klunk, *Neurobiol Aging.* **1998**, *19*, 145.
- [23] C. A. Mathis, B. J. Bacskai, S. T. Kajdasz, M. E. McLellan, M. P. Frosch, B. T. Hyman, D. P. Holt, Y. Wang, G. F. Huang, M. L. Debnath, W. E. Klunk, *Bioorg. Med. Chem. Lett.* **2002**, *12*, 295.
- [24] E. E. Nesterov, J. Skoch, B. T. Hyman, W. E. Klunk, B. J. Bacskai, T. M. Swager, *Angew. Chem. Int. Edit.* **2005**, *26*, 5452.
- [25] J. F. Poduslo, G. L. Curran, J. A. Peterson, D. J. McCormick, A. H. Fauq, M. A. Khan, T. M. Wengenack, *Biochem.* **2004**, *43*, 6064.
- [26] P. Hermann, J. Kotek: "Ten-membered Rings or Larger with One or More Nitrogen Atoms." in *Comprehensive Heterocyclic Chemistry III*, A. R. Katritzky, C. A. Ramsden, E. F. V. Scriven and R. J. K. Taylor, Elsevier, Oxford, 2008.
- [27] C. Wängler, B. Wängler, M. Eisenhut, U. Haberkorn, W. Mier, *Bioorg. Med. Chem.* **2008**, *16*, 2606.
- [28] A. Hamplová, P. Coufal, Z. Bosáková, F. Opekar, V. Kubíček, *Chem. Listy* **2008**, *102*, 194.
- [29] I. Mamedov, A. Mishra, G. Angelovski, H. A. Mayer, L. O. Palsson, D. Parker, N. K. Logothetis, *Dalton Trans.* **2007**, 5225.
- [30] W. Mier, J. Hoffend, S. Kramer, J. Schuhmacher, W. E. Hull, M. Eisenhut, U. Haberkorn, *Bioconjugate Chem.* **2005**, *16*, 237.
- [31] M. M. Vora, R. D. Finn, A. M. Emran, T. E. Boothe, P. J. Kothari, *J. Chromatogr.* **1986**, *369*, 187.
- [32] T. Arbughi, F. Bertani, R. Celeste, A. Grotti, S. Sillari, P. Tirone, *J. Chromatogr. B* **1998**, *713*, 415.
- [33] J. Künnmeyer, L. Terborg, S. Nowak, A. Scheffer, L. Telgmann, F. Tokmak, A. Günzel, G. Wiesmüller, S. Reichelt, U. Karst, *Anal. Chem.* **2008**, *80*, 8163.
- [34] S. Liu, Z. He, W. Y. Hsieh, P. E. Fanwick, *Inorg. Chem.* **2003**, *42*, 8831.

- [35] C. Li, W. T. Wong, *J. Org. Chem.* **2003**, *68*, 2956.
- [36] J. F. Desreux, *Inorg. Chem.* **1980**, *19*, 1319.
- [37] A. Dadabhoy, S. Faulkner, P. G. Sammes, *J. Chem. Soc., Perkin Trans.* **2002**, *2*, 348.
- [38] C. A. Mathis, Y. Wang, D. P. Holt, G. Huang, M. L. Debnath, W. E. Klunk, *J. Med. Chem.* **2003**, *46*, 2740.
- [39] V. R. Meyer, *Practical High Performance Liquid Chromatography* (3rd edition), Chichester, John Wiley & Sons, 2000.
- [40] A. Hamplová, *Separace polykarboxylátových derivátů cyklohexenu pomocí HPLC* (diplomová práce), PřF UK, 2007.
- [41] R. C. Graham, *Data Analysis for the Chemical Sciences – A Guide to Statistical Techniques*, VCH, Weinheim, 1993.
- [42] L. R. Snyder, J. J. Kirkland, J. L. Glajch, *Practical HPLC Method Development* (2nd edition), Wiley-Interscience, New York, 1997.
- [43] R. Lucena, S. Cardenas, M. Valcarcel, *Anal. Bioanal. Chem.* **2007**, *388*, 1663.
- [44] K. Petritis, I. Gillaizeau, C. Elfakir, M. Dreux, A. Petit, N. Bongibault, W. Luijten, *J. Sep. Sci.* **2002**, *25*, 593.
- [45] E. Paredes, S. E. Maestre, S. Prats, J. L. Todoli, *Anal. Chem.* **2006**, *78*, 6774.
- [46] I. S. Krull, Z. Deyl, H. Lingeman, *J. Chromatogr. B* **1994**, *659*, 1.
- [47] M. C. Prieto-Blanco, P. López-Mahía, P. Campíns-Falcó, *Anal. Chem.* **2009**, *81*, 5827.
- [48] I. S. Krull, M. E. Szulc, A. J. Bourque, F. X. Zhou, J. Yu, R. Strong, *J. Chromatogr. B* **1994**, *659*, 19.
- [49] I. Aichinger, G. Gübitz, J. W. Birks, *J. Chromatogr. A* **1990**, *523*, 163.
- [50] U. A. T. Brinkman, *Chromatographia* **1987**, *24*, 190.
- [51] O. R. Idowu, *J. Liq. Chrom.* **1993**, *16*, 2501.
- [52] I. Molnár-Perl, *J. Chromatogr. A* **2000**, *891*, 1.
- [53] D. Fekkes, *J. Chromatogr. B* **1996**, *682*, 3.
- [54] R. Schuster, *J. Chromatogr.* **1988**, *431*, 271.
- [55] M. P. Olson, L. R. Keating, W. R. LaCourse, *Anal. Chim. Acta* **2009**, *652*, 198.
- [56] J. T. Smith, *Electrophoresis* **1999**, *20*, 3078.
- [57] H. Wan, L. G. Blomberg, *J. Chromatogr. A* **2000**, *875*, 43.

- [58] V. Kašička, *Electrophoresis* **2006**, 27, 142.
- [59] Z. Deyl, R. Struzinsky, *J. Chromatogr. B* **1991**, 569, 63.
- [60] B. Verzola, C. Gelfi, P. G. Righetti, *J. Chromatogr. A* **2000**, 874, 293.
- [61] M. Gilges, M. H. Kleemiss, G. Schomburg, *Anal. Chem.* **1994**, 66, 2038.
- [62] P. Coufal, J. Zuska, T. van de Goor, V. Smith, B. Gaš, *Electrophoresis* **2003**, 24, 671.
- [63] H. Nishi, S. Terabe, *J. Chromatogr. A* **1996**, 735, 3.
- [64] T. Kaneta, H. Shiba, T. Imasaka, *J. Chromatogr. A* **1998**, 805, 295.
- [65] Z. Cobb, P. N. Shaw, L. L. Lloyd, N. Wrench, D. A. Barret, *J. Microcol. Sep.* **2001**, 13, 169.
- [66] C. Yu, F. Švec, J. M. J. Fréchet, *Electrophoresis* **2000**, 21, 120.
- [67] H. Bruckner, M. Hausch, *J. Chromatogr.* **1993**, 614, 7.
- [68] P. Hušek, *J. Chromatogr. B* **1998**, 717, 57.
- [69] Y. Yokoyama, T. Amaki, S. Horikoshi, H. Sato, *Anal. Sci.* **1997**, 13, 1963.
- [70] A. Fialaire, E. Postaire, R. Prognon, D. Pradeau, *J. Liq. Chromatogr.* **1993**, 16, 3003.
- [71] R. Hanczko, A. Jámbor, A. Perl, I. Molnár-Perl, *J. Chromatogr. A* **2007**, 1163, 25.
- [72] R. Checa-Moreno, E. Manzano, G. Mirón, L. F. Capitán-Vallvey, *J. Sep. Sci.* **2008**, 31, 3817.
- [73] A. Jámbor, I. Molnár-Perl, *J. Chromatogr. A* **2009**, 1216, 3064.
- [74] S. A. Cohen, D. P. Michaud, *Anal. Biochem.* **1993**, 211, 279.
- [75] M. T. Kelly, A. Blaise, M. Larroque, *J. Chromatogr. A* **2010**, 1217, 7385.
- [76] M. J. Friedman, *J. Agric. Food Chem.* **2004**, 52, 385.
- [77] D. Kutlán, J. Molnár-Perl, *J. Chromatogr. A* **2003**, 987, 311.
- [78] M. Puig-Deu, S. Buxaderas, *J. Chromatogr. A* **1994**, 685, 21.
- [79] V. Lozanov, S. Petrov, V. Mitev, *J. Chromatogr. A* **2004**, 1025, 201.
- [80] E. Valero, T. M. Berlanga, P. M. Roldán, C. Jiménez, I. Garcia, J. C. Mauricio, *J. Sci. Food. Agric.* **2005**, 85, 603.
- [81] M. A. Smith, G. P. Davies, *Plant Physiol.* **1985**, 78, 89.
- [82] L. Bosch, A. Alegría, R. Farré, *Journal of Chromatogr. B* **2006**, 831, 176.

- [83] K. Héberger, E. Csomos, L. Simon-Sarkadi, *J. Agric. Food. Chem.* **2003**, *51*, 8055.
- [84] S. Levin, E. Grushka, *Anal. Chem.* **1985**, *57*, 1830.
- [85] B. M. Polanuer, S. V. Ivanov, *J. Chromatogr. A* **1996**, *722*, 311.
- [86] G. Anderegg, F. Arnaud-Neu, R. Delgado, J. Felcman, K. Popov, *Pure Appl. Chem.* **2005**, *77*, 1445.
- [87] A. Bencini, A. Bianchi, E. García-España, M. Micheloni, J. A. Ramirez, *Coord. Chem. Rev.* **1999**, *188*, 97.
- [88] I. Lukeš, J. Kotek, P. Vojtíšek and P. Hermann, *Coord. Chem. Rev.* **2001**, *287*, 216.
- [89] V. Loreti, J. Bettmer, *Anal. Bioanal. Chem.* **2004**, *379*, 1050.
- [90] M. Sillanpaa, K. B. Raimo, M. L. Sihvonen, *Anal. Chim. Acta* **1995**, *303*, 187.
- [91] P. Laine, R. Matilainen, *Anal. Bioanal. Chem.* **2005**, *382*, 1601.
- [92] NIST Standard Reference Database 46 (Critically Selected Stability Constants of Metal Complexes), Version 7.0, 2003.
- [93] M. Kývala, I. Lukeš, *International Conference Chemometrics '95*, Pardubice, Czech Republic, 1995, pp 63. The full version of the OPIUM program is available (free of charge) on http://www.natur.cuni.cz/_kyvala/opium.html.
- [94] K. Petrikis, C. Elfakir, M. Dreux, *J. Chromatogr. A* **2002**, *961*, 9.
- [95] R. M. Callejón, A. M. Troncoso, M. L. Morales, *Talanta* **2010**, *81*, 1143.

ACKNOWLEDGEMENT

This thesis would not have been possible without my supervisor, Doc. P. Coufal, whose encouragement, guidance and support from the initial to the final level have been of great value for me. I am also grateful to my consultant, Doc. Z. Bosáková, for her advice and suggestions. Last but not least I would like to thank all colleagues from the separation team, who supported me in a number of ways during the four years of my dissertation work.

LIST OF PUBLICATIONS

1. **A. Kubíčková**, V. Kubíček, P. Coufal: *UV-VIS detection of amino acids in HPLC: on-line post-column solid-state derivatization with Cu(II) ions*, J. Sep. Sci. **34** (2011) DOI 10.1002/jssc.201100561.
2. **A. Kubíčková**, T. Křížek, P. Coufal, E. Wernersson, J. Heyda and P. Jungwirth: *Guanidinium Cations Pair with Positively Charged Arginine Side Chains in Water*, J. Phys. Chem. Lett. **2** (2011) 1387 – 1389.
3. E. Wernersson, J. Heyda, **A. Kubíčková**, T. Křížek, P. Coufal, P. Jungwirth: *Effect of association with sulfate on the electrophoretic mobility of polyarginine and polylysine*, J. Phys. Chem. B **114** (2010) 11934 – 11941, IF 3.471.
4. **A. Hamplová**, T. Křížek, V. Kubíček, Z. Bosáková, P. Coufal: *Comparison of HPLC and CZE methods for analysis of DOTA-like esters – reaction intermediates in synthesis of magnetic resonance contrast agents*, J. Sep. Sci. **33** (2010) 658 – 663, IF 2.551.
5. V. Kubíček, **A. Hamplová**, L. Maribe, S. Mameri, R. Ziessel, E. Jakab-Toth, L. Charbonniere: *Relaxation and luminescence studies on hydrated bipyridyl- and terpyridyl-based lanthanide complexes*, Dalton Transactions, **43** (2009) 9466 – 9474, IF 4.081.
6. **A. Hamplová**, P. Coufal, Z. Bosáková, F. Opekar, V. Kubíček: *HPLC separation of cyclen polycarboxylates using contactless conductivity detection*, Chem. listy, **102** (2008) 194 – 199, IF 0.717

PATENT APPLICATION

P. Coufal, **A. Kubičková**, V. Kubiček, M. Franc, J. Vojta, E. Tesařová, Z. Bosáková:
Post-column solid-state derivatization in HPLC, Industrial Property Office of the
Czech Republic, application number E106569, document number PV2010-845.

DECLARATION OF CO-AUTHORS

On behalf of the co-authors I declare that Mgr. Anna Kubíčková contributed substantially to paper 1 entitled „*UV-VIS detection of amino acids in HPLC: on-line post-column solid-state derivatization with Cu(II) ions.*“ Her share was 95 %.

On behalf of the co-authors I declare that Mgr. Anna Kubíčková contributed substantially to paper 4 entitled „*Comparison of HPLC and CZE methods for analysis of DOTA-like esters – reaction intermediates in synthesis of magnetic resonance contrast agents.*“ Her share was 90 %.

On behalf of the co-authors I declare that Mgr. Anna Kubíčková contributed substantially to paper 6 entitled „*HPLC separation of cyclen polycarboxylates using contactless conductivity detection.*“ Her share was 90 %.

Prague, October 2011

Doc. RNDr. Pavel Coufal, Ph.D.

On behalf of the co-authors I declare that Mgr. Anna Kubíčková contributed substantially to paper 2 entitled „*Guanidinium Cations Pair with Positively Charged Arginine Side Chains in Water.*“ Her share was 30 %.

On behalf of the co-authors I declare that Mgr. Anna Kubíčková contributed substantially to paper 3 entitled „*Effect of association with sulfate on the electrophoretic mobility of polyarginine and polylysine.*“ Her share was 20 %.

Prague, October 2011

Prof. Mgr. Pavel Jungwirth, DSc.

On behalf of the co-authors I declare that Mgr. Anna Kubíčková contributed substantially to paper 5 entitled „*Relaxation and luminescence studies on hydrated bipyridyl- and terpyridyl-based lanthanide complexes.*“ Her share was 10 %.

Prague, October 2011

RNDr. Vojtěch Kubíček, Ph.D.